A chaos study of fractional SIR epidemic model of childhood diseases

Shaher Momani, Ranbir Kumar, H. M. Srivastava, Sunil Kumar, & Samir Hadid

August 2021

Results in Physics 27 (2021) 104422

Contents lists available at ScienceDirect

Results in Physics

journal homepage: www.elsevier.com/locate/rinp

A chaos study of fractional SIR epidemic model of childhood diseases

Shaher Momani [a,b], Ranbir Kumar [c], H.M. Srivastava [d,e,g,h], Sunil Kumar [a,c,*], Samir Hadid [a,f]

[a] Nonlinear Dynamics Research Center (NDRC), Ajman University, Ajman, United Arab Emirates
[b] Department of Mathematics, Faculty of Science, University of Jordan, Amman, Jordan
[c] Department of Mathematics, National Institute of Technology, Jamshedpur 831014, Jharkhand, India
[d] Department of Mathematics and Statistics, University of Victoria, Victoria, British Columbia V8W 3R4, Canada
[e] Department of Medical Research, China Medical University Hospital, Taichung, 40402, Taiwan, Republic of China
[f] Department of Mathematics and Sciences, College of Humanities and Sciences, Ajman University, Ajman, United Arab Emirates
[g] Department of Mathematics and Informatics, Azerbaijan University, 71 Jeyhun Hajibeyli Street, AZ1007 Baku, Azerbaijan
[h] Section of Mathematics, International Telematic University Uninettuno, I-00186 Rome, Italy

ARTICLE INFO

Keywords:
SIR epidemic model
Laguerre wavelets
Operational matrix
Fractional-order differential equations (FDEs)
Fractional derivatives
Dynamical systems
Adams-Bashforth-Moulton method

ABSTRACT

Models of bio-mathematics are experimental systems that recreate aspects of human tissue function, diseases or virus. In this research, a new operational matrix based on the Laguerre wavelets is introduced for a arbitrary-order susceptible-infected-recovered (SIR) epidemic dynamical system of childhood diseases. An exact mechanism for the Riemann–Liouville arbitrary integral operator for the Laguerre wavelets is explained where the arbitrary-order derivative is assumed in the Liouville-Caputo style. Further, we use this operational matrix to convert the given dispute into a system of algebraic equations. The chaotic attractors for fractional-order SIR dynamical model are illustrated graphically by adopting the Adams–Bashforth-Moulton (ABM) scheme. Numerical simulations and results for the susceptible, infected and recovered peoples are carried out by using the Laguerre wavelets. Their behaviour with respect to time is seen to be the key features of this work. Moreover, we have compared the Laguerre wavelet solutions with the ABM solution for the truthfulness and applicability of the Laguerre wavelets scheme.

Introduction and motivation

Epidemiology is one of the most popular research areas of the biological sciences that investigate the design of health, sickness and other connected aspects at the population level. The conversation on "epidemiology" is assumed from the three Greek words, epi, demos and logos, which mean upon, public and study, respectively. This etymology signifies that the discussion on epidemiology appeals only to human populations (see [1]). Now-a-days the popular research area of contagious diseases has been one of the wealthy areas of applications and researches of mathematics in biological sciences. Contagious diseases obviously introduce great overloads of morbidity and mortality on the human race, as well as on non–human populations of focus to us. Hence, the capability to use formal models to minimize those overloads has attracted the attention of mathematicians and biologists (see [2]). Many researchers devoted themselves toward various established models in mathematics in order to investigate the spray of contagious diseases in the research area of mathematical biology (see, for example, [3–5]).

A given model in mathematics is a characterization of a system with the help of the mathematical mechanisms and language. The process of establishing models of mathematics is known as mathematical modelling. Now-a-days contagious diseases spread has prompted rich attention to public health analysis. Due to this reason, we will examine the modelling of contagious diseases and the analysis of their transmission in populations. But, according to the assumption made, mathematical modeling can be applied to any model of biological, physical and other related research areas. Mathematical systems play a significant role in analyzing the process of transmission of illnesses, in studying the effects of the various components involved, in making predictions about their behaviour, and providing distinct techniques with a view to controlling the propagation of the illness considered. In the past several years, modelling of contagious diseases of bio-mathematics by using the system of arbitrary-order differential equations (FDEs) has motivated remarkable consideration and attention. The bio-mathematics happens

* Corresponding author at: Nonlinear Dynamics Research Center (NDRC), Ajman University, Ajman, United Arab Emirates and Department of Mathematics, National Institute of Technology, Jamshedpur-831014, Jharkhand India. Tel.:+91-7870102516.
E-mail addresses: skiitbhu28@gmail.com, skumar.math@nitjsr.ac.in (S. Kumar).

https://doi.org/10.1016/j.rinp.2021.104422
Received 14 April 2021; Received in revised form 1 June 2021; Accepted 2 June 2021
Available online 11 June 2021

to be essential in the authentic sensitivity of the word such as about how things live, how things breathe, and how things die.

Now-a-days a wide consideration of various mathematical models of epidemics is that the population can be divided into a set of different compartments. These compartments are determined by observing the disease level. In the year 1927, the simplest model of the SIR (susceptible-infected-recovered) epidemic was first discovered by Kermack and McKendrick [6] which is one of the simplest compartmental systems, and various other models are derived from its basic form. The classical SIR epidemic model of childhood diseases is characterized by initial-value problems such as the following model:

$$\begin{cases} \mathscr{S}'(t) = (1-P)b - \beta\mathscr{S}\mathscr{I} - b\mathscr{S}, & \mathscr{S}(0)\geqslant 0, \\ \mathscr{I}'(t) = \beta\mathscr{S}\mathscr{I} - (\delta+\mu)\mathscr{I}, & \mathscr{I}(0)\geqslant 0, \\ \mathscr{R}'(t) = Pb + \delta I - \mu\mathscr{R}, & \mathscr{R}(0)\geqslant 0, \end{cases} \tag{1.1}$$

with the primary values $\mathscr{S}(0) = 0.92, \mathscr{I}(0) = 0.06$ and $\mathscr{R}(0) = 0.02$. In the above model (1.1), b is the constant birth percentage, μ is the natural death percentage, β is the average contact percentage, δ is the percentage recovery of the infected person, and P is the population of the people vaccinated at the birth time (see [7]). The SIR model consists of the following three groups (see [6,8]):

- Group $\mathscr{S}$ for the statistics of the susceptible people where all people are susceptible if they contract a disease, but are at risk of being infected at time t.
- Group $\mathscr{I}$ for the statistics of the infected people, where all people are infected by the disease and can transmit it to others at time t.
- Group $\mathscr{R}$ for the statistics of the recovered people, where all people are recovered from the disease at time t.

We found that childhood diseases are common and most dangerous epidemic infectious diseases of the human body. There are various infectious and non-infectious childhood diseases that it would be impossible to list them all in this research work. However, we will introduce some of the most common ones, including viral and bacterial infections as well as allergic and immunologic illnesses such as (for example) ear infections, glue ear, croup, hand, foot, and mouth diseases (see [9–15]). These diseases have more effect on children compared to adults. Childhood diseases have several essential features that make them apposite for their mathematical modelling. Many researchers devoted themselves to study about childhood diseases (see, for example, [16]). The effects of vaccination in childhood diseases were studied by Singh et al. [14]. The SIR epidemic model is the fundamental epidemic model among all epidemiological models. In the epidemic models, the births and deaths are ignored; therefore, only two possibilities of transitions are possible: infection and recovery. The SIR models are congruous to define the transmission diseases due to infections with perennial immunity such as chickenpox, measles, smallpox, HIV-AIDS, mumps, and so on (see [17–22]). Various types of epidemic models of biomathematics have been solved by using several different kinds of analytical and numerical methods by many authors, researchers and biologists including (for example) Haq et al. [17], Makinde [23], Arqub and Ajou [24], Ahmed et al. [25], and Kumar [26]. In the year 2017, a fractional model of infection and recovery SIR model under the appropriate limits was discussed (see, for details, [27]). Subsequently, an arbitrary order SIR epidemic system with non-linear incidence percentage was analysed (see [28]). In the year 2019, solutions of arbitrary-order SIR epidemic system was discussed by Hasan et al. [29]. Moreover, in the same year 2019, Srivastava and Günerhan [16] discussed the SIR epidemic system of childhood diseases.

In the past few years, fractional-order modelling has become an effective and thought-provoking field of investigation in various perspectives. There are various ways of illustrating arbitrary-order derivatives and integrals involving both singular and non-singular kernels (see [30–33]). The Mittag–Leffler function has played an important role in defining various kinds of fractional derivatives leading, in turn, to interesting theories of fractional calculus (FC). Indeed, during the last five years, the vital interests in the Mittag–Leffler function have considerably increased among scientists and engineers due to their frequent applications in engineering and real-world problems. For example, Baleanu and others developed and applied various new and interesting results in fractional calculus leading to the solutions of various real-world problems (see, for details, [34–39]). In the year 2016, Atangana and Baleanu developed a arbitrary derivative based on kernel involving the Mittag–Leffler function [40] and applied it to real-world problems of physical, biological, and medical sciences (see [36,41–47]). In the year 2020, Dumitru et al. [48] have further developed and discovered a new fractional-calculus operators, namely, the proportional Liouville-Caputo and the constant proportional Liouville-

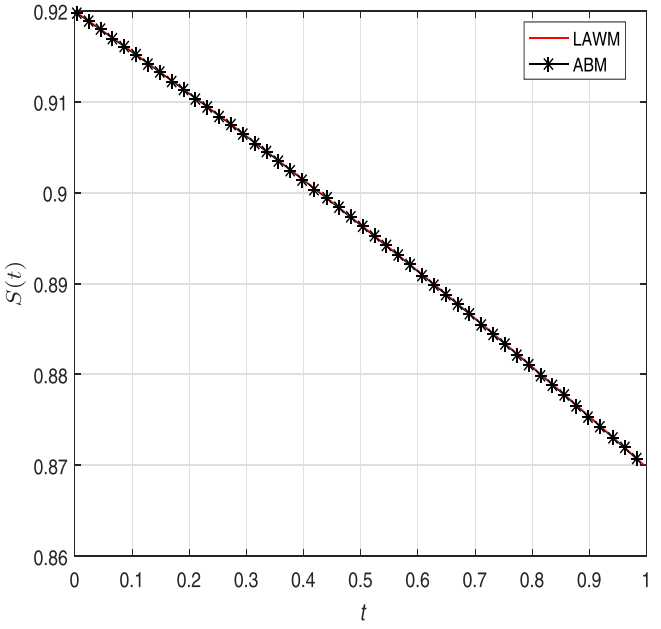

Fig. 1. Plot of the achieved LAWM and ABM solutions of the susceptible people for $M = 3$ and $k = 7$ when $\sigma = 1$.

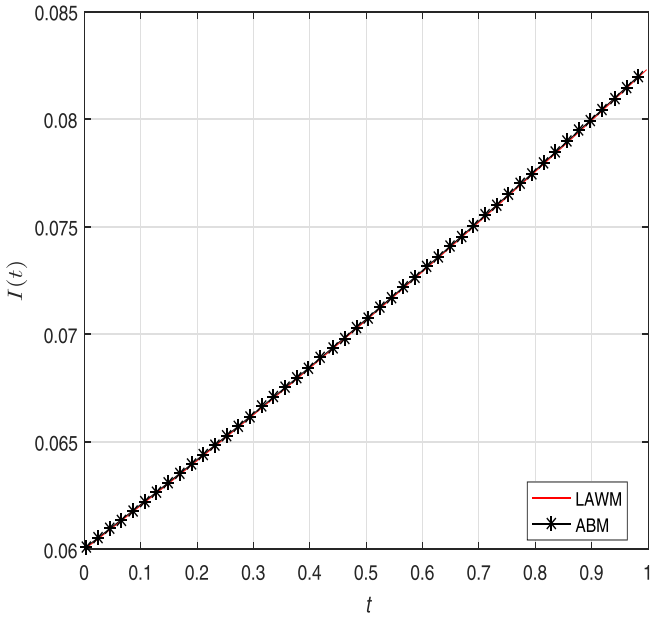

Fig. 2. Plot of the achieved LAWM and ABM solutions of the infected people for $M = 3$ and $k = 7$ when $\sigma = 1$.

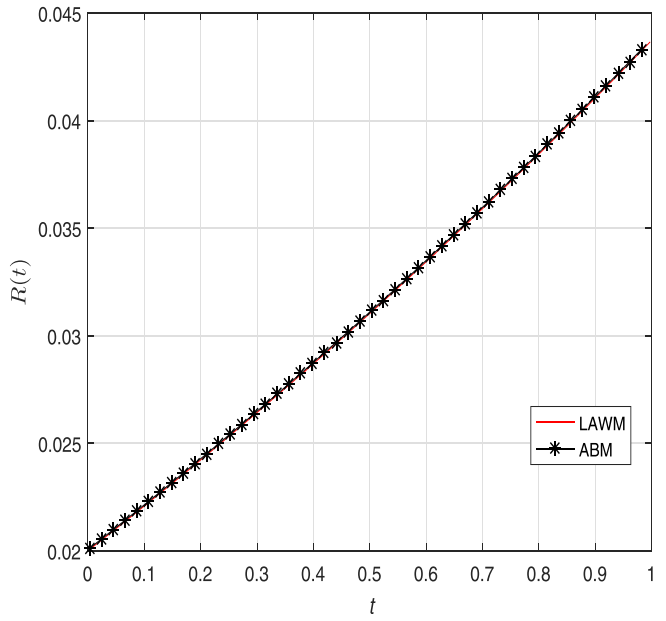

Fig. 3. Plot of the achieved LAWM and ABM solutions of the recovered people for $M = 3$ and $k = 7$ when $\sigma = 1$.

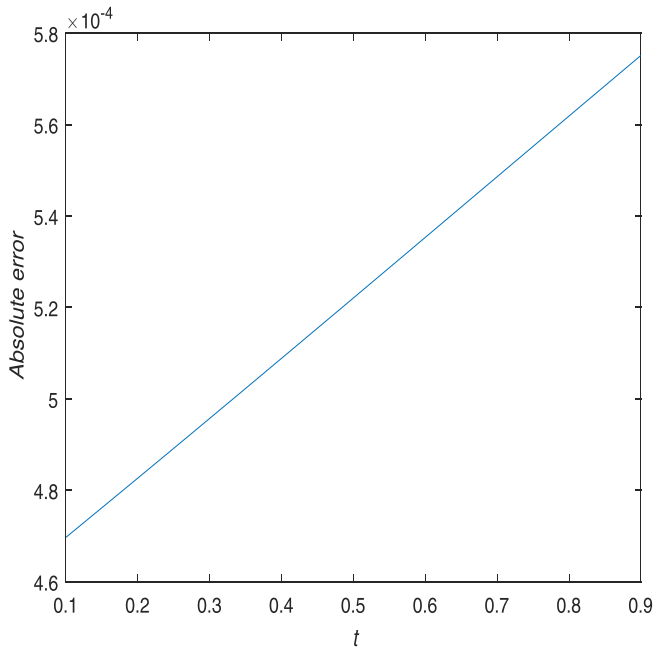

Fig. 4. Absolute error between the LAWM and ABM solutions for the susceptible people when $\sigma = 1$.

Caputo as well as their associated integral transforms. The applications of these new fractional-calculus operators, together with their basic properties, will be potentially useful for enhancing the works of scientists and researchers of fractional calculus (FC). The 'butterfly effects and graphs' have become a famous and thought-provoking slogan of chaos. The investigation of chaos is common in such disciplines of applied sciences as astronomy, meteorology, population biology, and economics [49]. Chaos is a property of dynamical systems which are of at least three different kinds. Chaos happens to be most easily defined in the mathematical dynamical systems (see [50,51]). Chaotic behaviour exists in various natural systems, heartbeat irregularities, including fluid flow, weather, climate and other dynamical systems of biological science. Theoretically, we can say that chaotic behaviour could not occur in the finite state machine because the state vectors would eventually be periodic (see [52]).

In various cases, it is very difficult to get analytical solutions of various arbitrary-order differential equations occurring in science and engineering. Wavelet methods are relatively popular and dominating trending methods in order to solve various kinds of fractional differential equations of arbitrary orders, which arise in science and engineering; these methods greatly contribute toward helping us to understand many nonlinear phenomena. Now-a-days constructions of wavelet methods based on orthogonal polynomials are popular in various research areas of applied mathematics. Wavelet methods based on the Legendre polynomials, the Bernstein polynomials, the Laguerre polynomials, the Gegenbauer polynomials, the Hermite polynomial, and the Chebyshev polynomials are constructed for solving differential-equation problems by many researchers in applied sciences and engineering (see, for details, [53–65]).

The essential target of the present effort is to a discussion of an skilful mechanism for solving a arbitrary-order SIR epidemic disease system which is based upon the Laguerre wavelets approximation. The exact principles for the Riemann–Liouville arbitrary integral operator associated with the Laguerre wavelets is determined here for the first time. Moreover, these principles are used here to convert the nonlinear FDEs into the structure of algebraic equations. Furthermore, the Adams–Bashforth-Moulton (ABM) mechanism is also explained for solving the same arbitrary-order SIR epidemic disease system. Moreover, the derived solutions are compared with those found by using the ABM mechanism for the certainty and appropriateness of the Laguerre wavelets method (see [66,67]). The arbitrary-order SIR epidemic system is characterized in the following manner:

$$\begin{cases} {}^{\mathrm{LC}}D_t^{\sigma}\mathscr{S}(t) = (1-P)b - \beta\mathscr{S}\mathscr{I} - b\mathscr{S}, \\ {}^{\mathrm{LC}}D_t^{\sigma}\mathscr{I}(t) = \beta\mathscr{S}\mathscr{I} - (\delta+\mu)\mathscr{I}, \\ {}^{\mathrm{LC}}D_t^{\sigma}\mathscr{R}(t) = Pb + \delta I - \mu\mathscr{R}, \end{cases} \tag{1.2}$$

together with the initial values $\mathscr{S}(0) = 0.92, \mathscr{I}(0) = 0.06$ and $\mathscr{R}(0) = 0.02$. The arbitrary-order time-derivative operator ${}^{\mathrm{LC}}D_t^{\sigma}$ is assumed here in the Liouville-Caputo (LC) style, the order of the derivative being σ $(0 < \sigma \leqslant 1)$. We also write (see [68]) ${}^{\mathrm{LC}}D_t^{\sigma} = \frac{d^{\sigma}}{dt^{\sigma}}$.

The rest of the proposed work is set up as follows. In part 2, we have discussed about the Laguerre wavelets and their properties. In part 3, an exact formula for the Riemann–Liouville (RL) fractional-order integral operator associated with the Laguerre wavelets is derived. Error analysis for accuracy of the derived solutions is given in part 4. Implementation of the Laguerre wavelet scheme and the Adams–Bashforth-Moulton scheme on the proposed epidemic model is considered in part 5. In part 6, we present the numerical simulation and discussions. Summary and conclusions are given in part 7. Finally, in part 8, we briefly indicate some scopes and motivations for related future researches.

Essential assumptions of the operators of fractional calculus (FC)

Here, in this part, we present a few essential definitions which are necessary for establishing our results [69,70].

Definition 1. (*see [69,71]*) The (left-sided) Riemann–Liouville (LC) arbitrary integral of order σ of a function $\Theta(t) \in C_{\sigma}$ $(0 < \sigma \leqslant 1)$ is described as follows:

$$I_t^{\sigma}\Theta\left(t\right) = \frac{1}{\Gamma(\sigma)} \int_0^t (t-\xi)^{\sigma-1}\, \Theta\left(\xi\right) d\xi \left(\sigma > 0; t > 0\right), \tag{2.1}$$

where $\Gamma(.)$ is the familiar (Euler's) Gamma function.

Definition 2. (*see [71]*) The Riemann–Liouville (RL) and the Liouville-Caputo (LC) arbitrary derivatives of order σ are described, respectively, as follows:

$$
{}^{\mathrm{RL}}D_t^{\sigma}\Theta\left(t\right) = \frac{d^m}{dt^m}\left(I_t^{m-\sigma}\Theta(t)\right)
$$

$$
= \begin{cases} \dfrac{d^m\Theta(t)}{dt^m} & (\sigma = m \in \mathbb{N}) \\ \dfrac{1}{\Gamma(m-\sigma)}\ \dfrac{d^m}{dt^m}\ \displaystyle\int_0^t \frac{\Theta(\xi)}{(t-\xi)^{\sigma-m+1}}\ d\xi & (0 \leqslant m-1 < \sigma < m) \end{cases}
$$

and

$$
{}^{\mathrm{LC}}D_t^{\sigma}\Theta\left(t\right) = I_t^{m-\sigma}\left(\frac{d^m}{dt^m}\ \Theta\left(t\right)\right)
$$

$$
= \begin{cases} \dfrac{d^m\Theta(t)}{dt^m} & (\sigma = m \in \mathbb{N}) \\ \dfrac{1}{\Gamma(m-\sigma)}\ \displaystyle\int_0^t \frac{\Theta^m(\xi)}{(t-\xi)^{\sigma-m+1}}\ d\xi & (0 \leqslant m-1 < \sigma < m), \end{cases}
$$

where $t > 0$ and $m \in \mathbb{N}$. These operators of fractional calculus have the following properties for $m-1 < \sigma \leqslant m$ $(m \in \mathbb{N})$ and $\Theta \in L_1[a,b]$ $(b > a)$

$$
\begin{cases} \left({}^{\mathrm{LC}}D_t^{\sigma} I_t^{\sigma}\Theta\right)(t) = \Theta(t) \\ \left(I_t^{\sigma}\,{}^{\mathrm{LC}}D_t^{\sigma}\Theta\right)\left(t\right) = \Theta\left(t\right) - \displaystyle\sum_{k=0}^{m-1}\Theta^k\left(0+\right)\ \frac{(t-a)^k}{k!}. \end{cases} \tag{1.2}
$$

The laguerre wavelets and their useful properties

The Laguerre wavelet $\psi_{nm}(t) = \psi(k,n,m,t)$ have four parameters, which are explained over $[0,t_l)$ by

$$
\psi_{nm}\left(t\right) = \begin{cases} 2^{k/2}\ \mathscr{L}_m\left(\dfrac{2^k}{t_l}t - 2n + 1\right) & \left(\dfrac{n-1}{2^{k-1}}t_l \leqslant t < \dfrac{n}{2^{k-1}}t_l\right) \\ 0 & (\text{otherwise}), \end{cases} \tag{3.1}
$$

where $n = 0, 1, \cdots, 2^{k-1}$ and $m = 0, 1, \cdots, M-1$. Here $\mathscr{L}_m\left(t\right) = \frac{1}{m!}L_m(t)\Big)$ and $L_m(t)$ is the orthogonal Laguerre polynomial of degree m in t with the weight function $\omega(t) = 1$ on the interval $[0, \infty)$, which satisfies this recursive relations:

$$
L_0\left(t\right) = 1, \quad L_1\left(t\right) = 1 - t \quad \text{and} \quad L_{m+2}\left(t\right)
$$

$$
= \frac{(2m+3-t)L_{m+1}(t) - (m+1)L_m(t)}{m+2},
$$

where

$$
m \in \mathbb{N}_0 := \mathbb{N} \cup \{0\} = \{0, 1, 2, \cdots\}.
$$

The general formula for the Laguerre polynomials $L_m(t)$ is characterized as follows (see [72]):

$$
L_m\left(t\right) = \sum_{r=0}^{m} \frac{(-1)^r\, m!}{(m-r)!\,(r!)^2}\ t^r \qquad \left(m \in \mathbb{N}_0\right). \tag{3.2}
$$

Further, we let $\Omega_{k,M}$ be the space spanned by the Laguerre wavelets, that is,

$$
\begin{aligned} \Omega_{k,M} = &\ \operatorname{span}\left\{\psi_{1,0}, \psi_{2,0}, \cdots, \psi_{2^{k-1},0}, \psi_{1,1}, \cdots, \psi_{2^{k-1},1}, \cdots, \psi_{2^{k-1},M-1}\right\} \\ \subseteq &\ L^2(0,1). \end{aligned}
$$

Let Θ be member of $L^2(0,1)$ which has a unique best approximation in $\Omega_{k,M}$ such that

$$
P_M^{2^{k-1}}\Theta \in \Omega_{k,M}.
$$

Then, since

$$
P_M^{2^{k-1}}\Theta \in \Omega_{k,M}
$$

is the unique best approximation of Θ, there exist the following unique coefficients:

$$
\Delta_{1,0}, \Delta_{2,0}, \cdots, \Delta_{2^{k-1},0}, \Delta_{1,1}, \cdots, \Delta_{2^{k-1},1}, \cdots, \Delta_{2^{k-1},M-1}
$$

such that

$$
\Theta\left(t\right) \simeq \left(P_M^{2^{k-1}}\Theta\right)\left(t\right) = \sum_{n=1}^{2^{k-1}}\sum_{m=0}^{M-1}\Delta_{n,m}\psi_{n,m}\left(t\right) = C^T\Psi\left(t\right),
$$

The vectors C and Ψ are defined by

$$
C^T = \left[\Delta_{1,0}, \Delta_{2,0}, \cdots, \Delta_{2^{k-1},0}, \Delta_{1,1}, \cdots, \Delta_{2^{k-1},1}, \Delta_{2^{k-1},M-1}\right]
$$

and

$$
\Psi = \left[\psi_{1,0}, \psi_{2,0}, \cdots, \psi_{2^{k-1},0}, \psi_{1,1}, \cdots, \psi_{2^{k-1},1}, \cdots, \psi_{2^{k-1},M-1}\right]^T.
$$

Further, the matrix of the Laguerre wavelets is given as follows:

$$
\underset{\widehat{m}\times\widehat{m}=}{\Phi}\left[\Psi\left(\frac{2i-1}{2m}t_l\right)\right] \qquad \left(i=1,2,\ldots,2^{k-1}M\right)
$$

and

$$
\Phi_{6\times6} = \begin{pmatrix} 2.0000 & 2.0000 & 2.0000 & 0 & 0 & 0 \\ 0 & 0 & 0 & 2.0000 & 2.0000 & 2.0000 \\ 3.3333 & 2.0000 & 0.6667 & 0 & 0 & 0 \\ 0 & 0 & 0 & 3.3333 & 2.0000 & 0.6667 \\ 2.5556 & 1.0000 & -0.1111 & 0 & 0 & 0 \\ 0 & 0 & 0 & 2.5556 & 1.0000 & -0.1111 \end{pmatrix}
$$

$\Phi_{6\times6}$ being the Laguerre wavelet matrix at the collocations points $\frac{2i-1}{2\widehat{m}}t_l$ when $t_l = 1$.

Convergence analysis of Laguerre wavelets approximation

.

Theorem 1. *Let $\Theta(t) \in L^2[0,t_l]$ be the function and $\Theta_0(t) \in \Theta_{k,M}$ is the approximation of $\Theta(t)$ then*

$$
\left\|\epsilon_{\Theta}\right\| = \left\|\Theta(t) - \Theta_0(t)\right\| < \frac{\Upsilon t_l^{\frac{2M+1}{2}}}{M!\sqrt{2M+1}}.
$$

Proof. Let $\Theta^{(i)}(t)$ be the continuous function, where $i = 0, 1, 2, \ldots M$. Then there exist $\Upsilon \in \mathbb{N}$ such that

$$
\Theta^{(i)}\left(t\right) < \Upsilon, \quad \forall\ t \in \left[0, t_l\right].
$$

Then by Taylor's formula

$$
\Theta\left(t\right) = \sum_{i=0}^{M-1}\frac{\Theta^i(0)t^i}{i!} + \frac{\Theta^{(M)}(\xi)}{M!}t^M, \quad \text{where } \xi \in \left[0, t_l\right].
$$

Since, $\{\psi_{nm}(t)\}$ is the family of piecewise function. As $\Omega_{k,M} = span\{\psi_{nm}(t)\}$, therefore

$$
\sum_{0}^{M-1}\frac{\Theta^{(i)}(0)t^i}{i!} \in \Omega_{k,M},
$$

as $\Theta_0(t)$ is the best approximation of $\Theta(t)$ out of $\Omega_{k,M}$, then

$$\|\epsilon_\Theta\| = \|\Theta(t) - \Theta_0(t)\| \leqslant \|\Theta(t) - \sum_0^{M-1} \frac{\Theta^{(i)}(0)t^i}{i!}\| = \|\frac{\Theta^{(M)}(\xi)t^M}{M!}\|$$

$$= \left(\int_0^{t_l} \left(\frac{\Theta^{(M)}(\xi)t^M}{M!} \right)^2 \right)^{\frac{1}{2}} < \left(\frac{\Upsilon^2 t_l^{2M+1}}{(M!)^2(2M+1)} \right)^{\frac{1}{2}} = \frac{\Upsilon t_l^{\frac{2M+1}{2}}}{M!\sqrt{2M+1}}$$

where $t_l \in \mathbb{N}$ is the fixed number and when M is sufficiently large then $\|\epsilon_\Theta\| \to 0$. Hence Laguerre wavelets approximation is convergent. □

The Riemann–Liouville fractional integral operator for the laguerre wavelets

In this section, we derive the operational matrix for the Laguerre wavelets without adopting block pulse functions. For this analysis, we apply the integral operator I_t^σ directly into $\Psi(t)$ as follows:

$$I_t^\sigma \Psi(t) = Q(t,\sigma) = \left[I_t^\sigma \psi_{1,0}, I_t^\sigma \psi_{2,0}, \cdots, I_t^\sigma \psi_{2^{k-1},0}, I_t^\sigma \psi_{1,1}, \cdots, I_t^\sigma \psi_{2^{k-1},1}, \cdots, I_t^\sigma \psi_{2^{k-1},M-1} \right]^T.$$

Hence, clearly, we have

$$\psi_{nm}(t) = \frac{2^{k/2}}{m!}\, \mu_{\frac{n-1}{2^{k-1}}t_l}(t) 2^{k/2} L_m\left(\frac{2^k}{t_l}t - 2n + 1\right) - \frac{2^{k/2}}{m!}\mu_{\frac{n}{2^{k-1}}t_l}(t) 2^{k/2} L_m\left(\frac{2^k}{t_l}t - 2n + 1\right), \tag{4.1}$$

where

$$\mu_a(t) = \begin{cases} 1 & (t \geqslant a) \\ 0 & (t < a). \end{cases}$$

We now proceed to apply the Laplace transform to the above equation (4.1). We thus find that

$$\begin{aligned}
\psi_{nm}(t) &= \frac{2^{k/2}}{m!}\mathscr{L}\left\{ \mu_{\frac{n-1}{2^{k-1}}t_l}(t) L_m\left(\frac{2^k}{t_l}t - 2n + 1\right) \right\} \\
&\quad - \frac{2^{k/2}}{m!}\mathscr{L}\left\{ \mu_{\frac{n}{2^{k-1}}t_l}(t) L_m\left(\frac{2^k}{t_l}t - 2n + 1\right) \right\} \\
&= \frac{2^{k/2}}{m!}\mathscr{L}\left\{ \mu_{\frac{n-1}{2^{k-1}}t_l}(t) L_m\left(\frac{2^k}{t_l}\left(t - \frac{n-1}{2^{k-1}}t_l\right) - 1\right) \right\} \\
&\quad - \frac{2^{k/2}}{m!}\mathscr{L}\left\{ \mu_{\frac{n}{2^{k-1}}t_l}(t) L_m\left(\frac{2^k}{t_l}\left(t - \frac{n}{2^{k-1}}t_l\right) + 1\right) \right\} \\
&= \frac{2^{k/2}}{m!} e^{-\frac{n-1}{2^{k-1}}st_l} \mathscr{L}\left\{ L_m\left(\frac{2^k}{t_l}t - 1\right) \right\} - \frac{2^{k/2}}{m!} e^{-\frac{n}{2^{k-1}}st_l} \mathscr{L}\left\{ L_m\left(\frac{2^k}{t_l}t + 1\right) \right\}.
\end{aligned}$$

Now, from the assumptions of the Laguerre polynomials in the Eq. (3.2), we get

$$\begin{aligned}
\mathscr{L}\{\psi_{n,m}(t)\} &= \frac{2^{k/2}}{m!} e^{-\frac{n-1}{2^{k-1}}st_l} \mathscr{L}\left\{ \sum_{r=0}^{m} \frac{(-1)^r m!}{(m-r)!\,(r!)^2} \left(\frac{2^k}{t_l}t - 1\right)^r \right\} \\
&\quad - \frac{2^{k/2}}{m!} e^{-\frac{n}{2^{k-1}}st_l} \mathscr{L}\left\{ \sum_{r=0}^{m} \frac{(-1)^r m!}{(m-r)!\,(r!)^2} \left(\frac{2^k}{t_l}t + 1\right)^r \right\} \\
&= \frac{2^{k/2}}{m!} e^{-\frac{n-1}{2^{k-1}}st_l} \sum_{r=0}^{m} \frac{(-1)^r m!}{(m-r)!\,(r!)^2} \mathscr{L}\left\{ \left(\frac{2^k}{t_l}t - 1\right)^r \right\} \\
&\quad - \frac{2^{k/2}}{m!} e^{-\frac{n}{2^{k-1}}st_l} \sum_{r=0}^{m} \frac{(-1)^r m!}{(m-r)!\,(r!)^2} \mathscr{L}\left\{ \left(\frac{2^k}{t_l}t + 1\right)^r \right\} \\
&= \frac{2^{k/2}}{m!} e^{-\frac{n-1}{2^{k-1}}st_l} \sum_{r=0}^{m} \frac{(-1)^r m!}{(m-r)!\,(r!)^2} \mathscr{L}\left\{ \sum_{i=0}^{r} \binom{r}{i} (-1)^i \left(\frac{2^k}{t_l}t\right)^{r-i} \right\} \\
&\quad - \frac{2^{k/2}}{m!} e^{-\frac{n}{2^{k-1}}st_l} \sum_{r=0}^{m} \frac{(-1)^r m!}{(m-r)!\,(r!)^2} \mathscr{L}\left\{ \sum_{i=0}^{r} \binom{r}{i} \left(\frac{2^k}{t_l}t\right)^{r-i} \right\}
\end{aligned}$$

Next, from the definition of the Riemann–Liouville (RL) fractional integral, we get

$$\begin{aligned}
\mathscr{L}\left\{ I_t^\sigma \psi_{n,m}\left(t\right) \right\} &= \mathscr{L}\left\{ \frac{t^{\sigma-1}}{\Gamma(\sigma)} * \psi_{n,m}\left(t\right) \right\} \\
&= \frac{2^{k/2}}{m!}\, e^{-\frac{n-1}{2^{k-1}}st_l} \sum_{r=0}^{m} \sum_{i=0}^{r} \frac{(-1)^r\, m!}{(m-r)!\,(r!)^2}\, \frac{r!}{i!}\, (-1)^i \left(\frac{2^k}{t_l}\right)^{r-i} \\
&\quad \frac{1}{s^{r-i+\sigma+1}} - \frac{2^{k/2}}{m!} e^{-\frac{n}{2^{k-1}}st_l} \sum_{r=0}^{m} \sum_{i=0}^{r} \frac{(-1)^r\, m!}{(m-r)!\,(r!)^2} \\
&\quad \frac{r!}{i!} \left(\frac{2^k}{t_l}\right)^{r-i} \frac{1}{s^{r-i+\sigma+1}},
\end{aligned} \tag{4.2}$$

which, by taking the inverse Laplace transform of both sides (4.2), can be written

$$\begin{aligned}
&= \frac{2^{k/2}}{m!} \sum_{r=0}^{m} \sum_{i=0}^{r} \frac{(-1)^{r+i}\, m!}{(m-r)!\,(r!)^2}\, \frac{r!}{i!} \left(\frac{2^k}{t_l}\right)^{r-i} \mu_{\frac{n-1}{2^{k-1}}t_l}\left(t - \frac{n-1}{2^{k-1}}t_l\right)^{r-i+\sigma} \\
&\quad \frac{1}{\Gamma(r-i+\sigma+1)} - \frac{2^{k/2}}{m!} \sum_{r=0}^{m} \sum_{i=0}^{r} \frac{(-1)^r\, m!}{(m-r)!\,(r!)^2}\, \frac{r!}{i!} \left(\frac{2^k}{t_l}\right)^{r-i} \\
&\quad \mu_{\frac{n}{2^{k-1}}t_l}\left(t - \frac{n}{2^{k-1}}t_l\right)^{r-i+\sigma} \frac{1}{\Gamma(r-i+\sigma+1)}.
\end{aligned} \tag{4.3}$$

We thus obtain

$$I_t^\sigma \psi_{nm}\left(t\right) = \begin{cases} 0 & \left(0 \leqslant t < \frac{n-1}{2^{k-1}}t_l\right) \\ 2^{k/2}\, \xi\left(n,m\right)\left(t - \frac{n-1}{2^{k-1}}\right)^\sigma & \left(\frac{n-1}{2^{k-1}}t_l \leqslant t < \frac{n}{2^{k-1}}t_l\right) \\ 2^{k/2}\, \xi\left(n,m\right)\left(t - \frac{n-1}{2^{k-1}}\right)^\sigma - 2^{k/2}\overline{\xi}\left(n,m\right)\left(t - \frac{n}{2^{k-1}}\right)^\sigma & \left(\frac{n}{2^{k-1}}t_l \leqslant t < t_l\right), \end{cases} \tag{4.4}$$

where

$$\xi\left(n,m\right)=\frac{1}{m!}\sum_{r=0}^{m}\sum_{i=0}^{r}\frac{(-1)^{r+i}\,m!}{(m-r)!(r!)^2}\;\frac{r!}{i!}\left(\frac{2^k}{t_l}\right)^{r-i}\left(t-\frac{n-1}{2^{k-1}}t_l\right)^{r-i}\frac{1}{\Gamma(r-i+\sigma+1)} \tag{4.5}$$

and

$$\overline{\xi}\left(n,m\right)=\frac{1}{m!}\sum_{r=0}^{m}\sum_{i=0}^{r}\frac{(-1)^{r}\,m!}{(m-r)!(r!)^2}\;\frac{r!}{i!}\left(\frac{2^k}{t_l}\right)^{r-i}\left(t-\frac{n}{2^{k-1}}t_l\right)^{r-i}\frac{1}{\Gamma(r-i+\sigma+1)}. \tag{4.6}$$

If, we now choose $k=2, M=3$ and $\sigma=0.5$, then we obtain the operational matrix as follows:

$$Q_{6\times6}^{0.5}=\begin{pmatrix}0.6515 & 1.1284 & 1.4567 & 1.0722 & 0.8260 & 0.7040\\ 0 & 0 & 0 & 0.6515 & 1.1284 & 1.4567\\ 1.1582 & 1.5045 & 1.2949 & 0.9108 & 0.7523 & 0.6583\\ 0 & 0 & 0 & 1.1582 & 1.5045 & 1.2949\\ 0.9326 & 0.9967 & 0.6609 & 0.4714 & 0.4101 & 0.3659\\ 0 & 0 & 0 & 0.9326 & 0.9967 & 0.6609\end{pmatrix}.$$

The above matrix is the operational matrix of the Laguerre wavelets.

Stability analysis of the arbitrary-Order SIR epidemic model

In this part, we return to the proposed arbitrary-order SIR model for its stability analysis. Indeed we have

$$\begin{cases}{}^{LC}D_t^{\sigma}\mathscr{S}(t)=(1-P)b-\beta\mathscr{S}\mathscr{I}-b\mathscr{S},\\ {}^{LC}D_t^{\sigma}\mathscr{I}(t)=\beta\mathscr{S}\mathscr{I}-(\delta+\mu)\mathscr{I},\\ {}^{LC}D_t^{\sigma}\mathscr{R}(t)=Pb+\delta\mathscr{I}-\mu\mathscr{R}.\end{cases} \tag{5.1}$$

In order to achieve the equilibrium points of the arbitrary-order SIR epidemic system, let us assume that

$$\begin{cases}(1-P)b-\beta\mathscr{S}\mathscr{I}-b\mathscr{S}=0,\\ \beta\mathscr{S}\mathscr{I}-(\delta+\mu)\mathscr{I}=0,\\ Pb+\delta\mathscr{I}-\mu\mathscr{R}=0.\end{cases} \tag{5.2}$$

Therefore, the equilibrium points of the system are $E_0\left\{\left(1-P\right),0,\frac{Pb}{\mu}\right\}$ and $E_1(\mathscr{S}_1,\mathscr{I}_1,\mathscr{R}_1)$, where

$$\mathscr{S}_1=\frac{\mu+\delta}{\beta},$$

$$\mathscr{I}_1=\frac{(1-P)b}{\mu+\delta}-\frac{b}{\beta}$$

and

$$\mathscr{R}_1=\frac{Pb}{\mu}+\frac{\delta}{\mu}\left[\frac{(1-P)b}{\mu+\delta}-\frac{b}{\beta}\right].$$

The Jacobian matrix for the system at the equilibrium point $\overline{E}\left(\overline{\mathscr{S}},\overline{\mathscr{I}},\overline{\mathscr{R}}\right)$ is given as follows:

$$J\left(\overline{E}\right)=\begin{pmatrix}-\left(\beta\overline{\mathscr{I}}+b\right) & -\beta\overline{\mathscr{S}} & 0\\ \beta\overline{\mathscr{I}} & \beta\overline{\mathscr{S}}-\left(\mu+\delta\right) & 0\\ 0 & \delta & -\mu\end{pmatrix}. \tag{5.3}$$

The characteristic polynomial of the above Jacobian matrix 5.3 is presented by

$$P\left(\lambda\right)=\lambda^3+\lambda^2\left(b+\delta+2\mu-\beta\overline{\mathscr{S}}-\beta\overline{\mathscr{I}}\right)+\lambda\left(b\delta+2b\mu+\delta\mu+\mu^2-b\beta\overline{\mathscr{S}}-\beta\delta\overline{\mathscr{I}}-\beta\mu\overline{\mathscr{S}}+2\beta\mu\overline{\mathscr{I}}\right)+\left(\beta\mu^2\overline{\mathscr{I}}+b\delta\mu-b\beta\mu\overline{\mathscr{I}}+\beta\delta\mu\overline{\mathscr{I}}+b\mu^2\right). \tag{5.4}$$

We now let

$$\begin{aligned}\xi_1&=\left(b+\delta+2\mu-\beta\overline{\mathscr{S}}-\beta\overline{\mathscr{I}}\right),\\ \xi_2&=\left(b\delta+2b\mu+\delta\mu+\mu^2-b\beta\overline{S}-\beta\delta\overline{\mathscr{I}}\beta\mu\overline{\mathscr{S}}+2\beta\mu\overline{\mathscr{I}}\right),\\ \xi_3&=\left(\beta\mu^2\overline{\mathscr{I}}+b\delta\mu-b\beta\mu\overline{\mathscr{S}}+\beta\delta\mu\overline{\mathscr{I}}+b\mu^2\right).\end{aligned}$$

Then the discriminant of Eq. 5.4 is characterized as follows:

$$D(\lambda)=18\xi_1\xi_2\xi_3+(\xi_1\xi_2)^2-4\xi_3\xi_1^3-4\xi_2^3-27\xi_3^2. \tag{5.5}$$

If we take the parameter values $P=0.3$, $b=0.1$, $\beta=0.75$, $\delta=0.35$ and $\mu=0.2$, then all of the characteristics values occur with the negative sign. Thus, by the Routh-Hurwitz condition [73,74] E_0 is locally asymptotically stable. Again, if we take the parameter values $P=0.05$, $b=0.01$, $\beta=0.8$, $\delta=0.35$ and $\mu=0.05$. Then the characteristic roots of Eq. 5.4 at E_1 are $\lambda_{1,2}=-0.0095\pm0.0594i$ and $\lambda_3=-0.0500$. Here the absolute value of $\arg(\lambda_{1,2})$ is 1.4122. So, clearly, E_1 is stable for $\sigma<0.8990$.

Numerical methods for the arbitrary-Order SIR epidemic model

In this part of our work, two different numerical schemes have been formulated for the approximations of arbitrary-order SIR epidemic system with the Liouville-Caputo derivative operator. Further, our aim is to employ the LAW and ABM mechanisms, each of which has been tested in terms of truthfulness and reliability to handle any kind of dynamical models of biological and medical sciences.

The Laguerre wavelets for arbitrary-order SIR epidemic system

The main focus of this subsection is to represent the arbitrary-order SIR epidemic models by using different methods. In order to elucidate the solution procedure of the Laguerre wavelet mechanism, let us assume the following nonlinear arbitrary-order SIR epidemic system of childhood diseases in biological sciences as follows:

$$\begin{cases}{}^{LC}D_t^{\sigma}\mathscr{S}(t)=C_1^T\Psi(t),\\ {}^{LC}D_t^{\sigma}\mathscr{I}(t)=C_2^T\Psi(t),\\ {}^{LC}D_t^{\sigma}\mathscr{R}(t)=C_3^T\Psi(t),\end{cases} \tag{6.1}$$

where

$$C_i^T=\left[\Delta_{1,0}^i,\Delta_{2,0}^i,\cdots,\Delta_{2^{k-1},0}^i,\Delta_{1,1}^i,\cdots,\Delta_{2^{k-1},1}^i,\cdots,\Delta_{2^{k-1},M-1}^i\right]$$

are the unknown parameters to be determined and $i=1,2,3$. Now, for the solution of above arbitrary-order SIR epidemic system, we have applied arbitrary integral operator to Eq. (6.1), so that

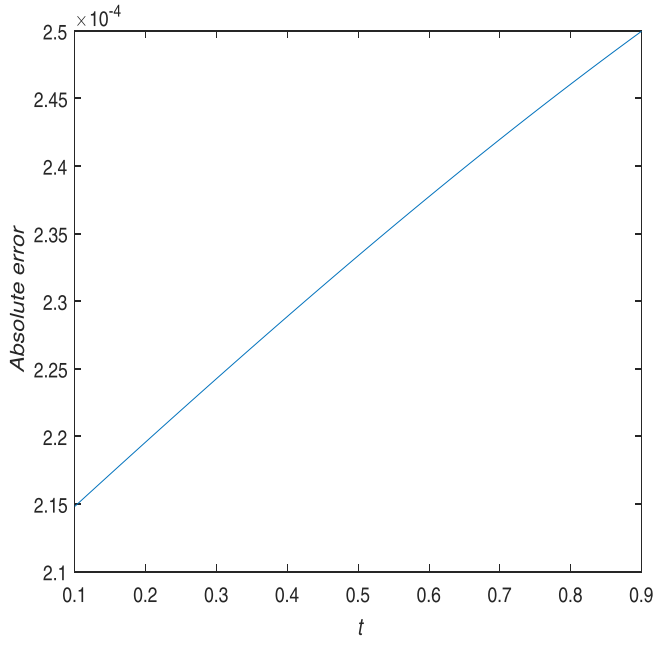

Fig. 5. Absolute error between the LAWM and ABM solutions for the infected people when $\sigma = 1$.

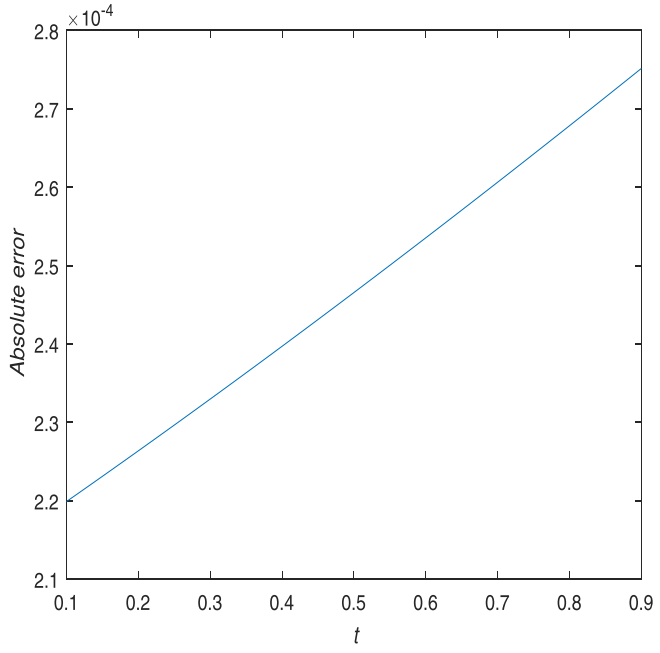

Fig. 6. Absolute error between the LAWM and ABM solutions for the recovered people when $\sigma = 1$.

$$\begin{cases} ({}_{t}^{\sigma LC}D_{t}^{\sigma})\mathscr{S} = \mathscr{S}(t) - S(0) = C_1^T Q(t,\sigma), \\ ({}_{t}^{\sigma LC}D_{t}^{\sigma})\mathscr{I} = \mathscr{I}(t) - I(0) = C_2^T Q(t,\sigma), \\ ({}_{t}^{\sigma LC}D_{t}^{\sigma})\mathscr{R} = \mathscr{R}(t) - R(0) = C_3^T Q(t,\sigma). \end{cases} \tag{6.2}$$

We then find that

$$\begin{cases} \mathscr{S}(t) = \mathscr{S}(0) + C_1^T Q(t,\sigma), \\ \mathscr{I}(t) = \mathscr{I}(0) + C_2^T Q(t,\sigma), \\ \mathscr{R}(t) = \mathscr{R}(0) + C_3^T Q(t,\sigma), \end{cases} \tag{6.3}$$

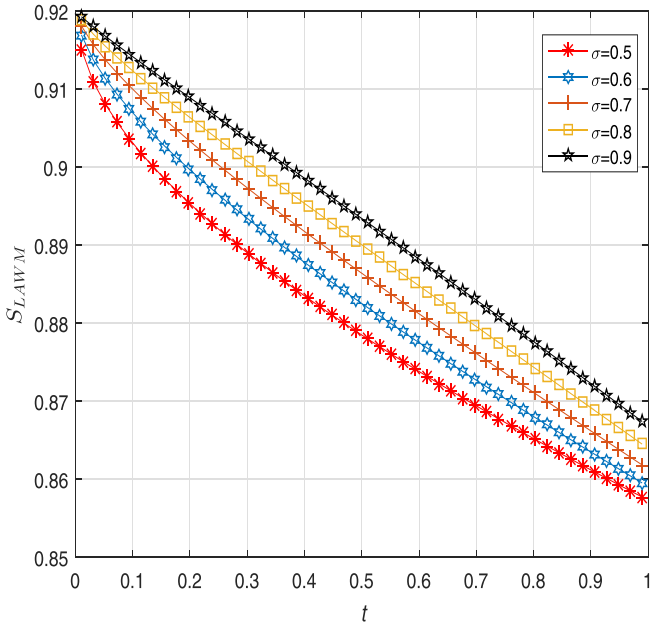

Fig. 7. Plot of the susceptible people for different values of σ.

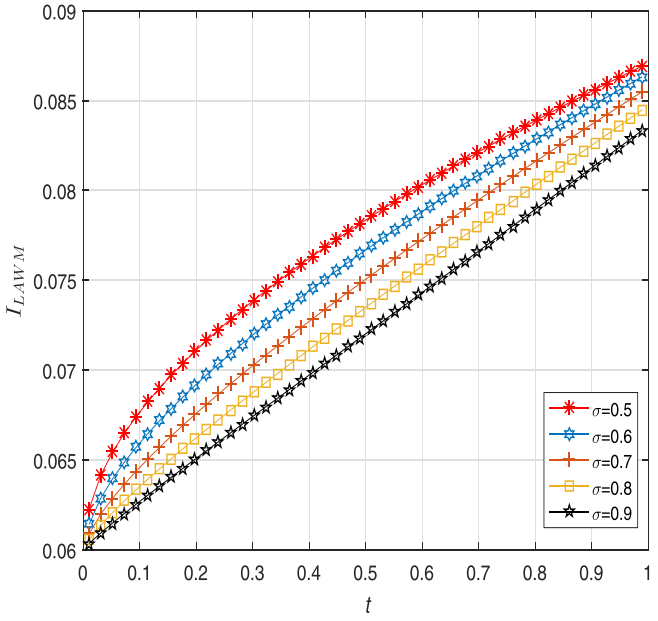

Fig. 8. Plot of the infected people for different values of σ.

where only C_i^T are the unknown parameters to be determined. Now, upon putting the above values of $\mathscr{S}(t), \mathscr{I}(t)$ and $\mathscr{R}(t)$ into the Eq. (1.2) and by adopting the collocation points $\frac{2i-1}{2\widehat{m}}$, we can archive the structure of the nonlinear algebraic equations with $3\widehat{m}$ number of the unknown parameters to be determined. Our next target is to calculate the solution of the resulting algebraic equations by adopting the Newton iteration technique. We can first ascertain the unknown parameter Laguerre coefficients and then use them into the Eq. (6.3) which is the required solution.

The Adams–Bashforth-Moulton (ABM) method for fractional-order SIR epidemic model

The ABM scheme provides very attractive numerical technique for

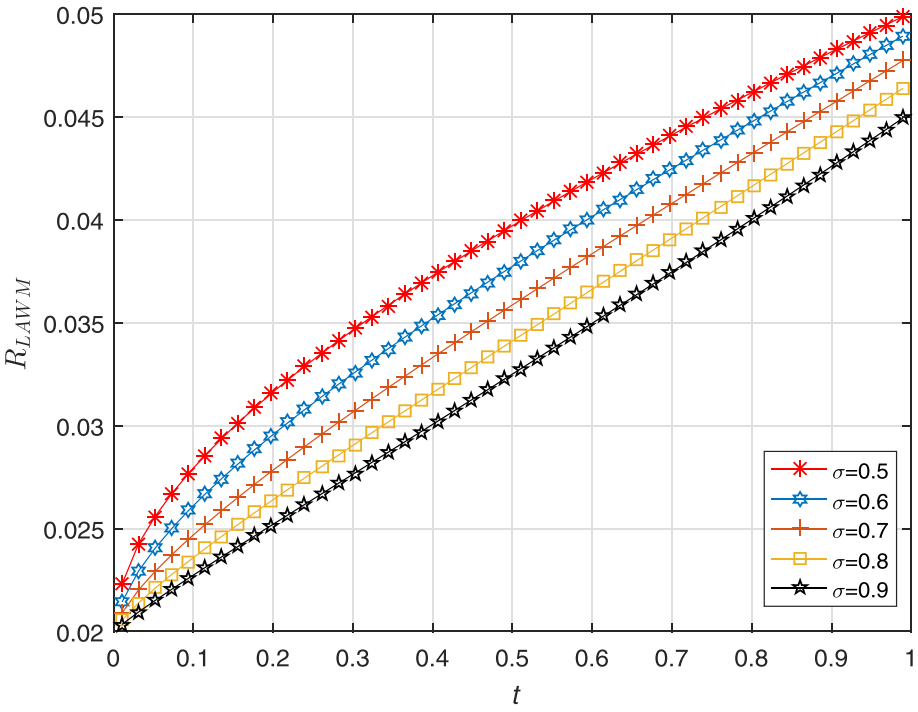

Fig. 9. Plot of the recovered people for different values of σ.

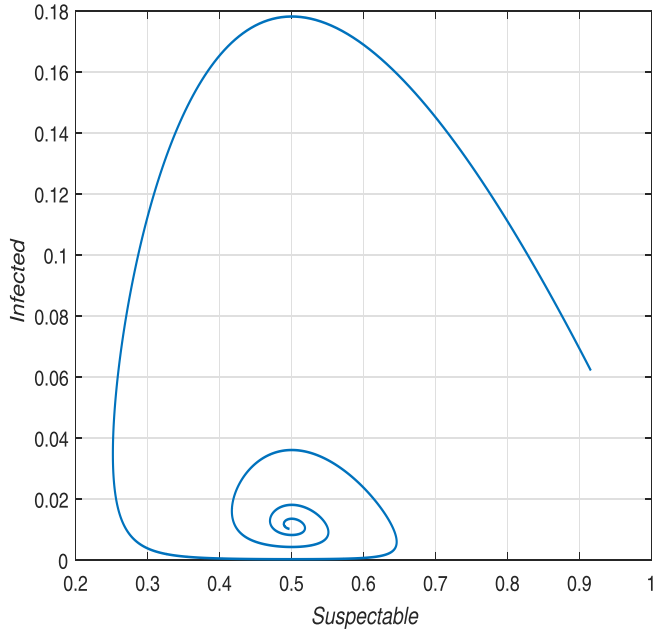

Fig. 10. Behaviour of the susceptible and the infected peoples for Case 1 when $\sigma = 0.9$.

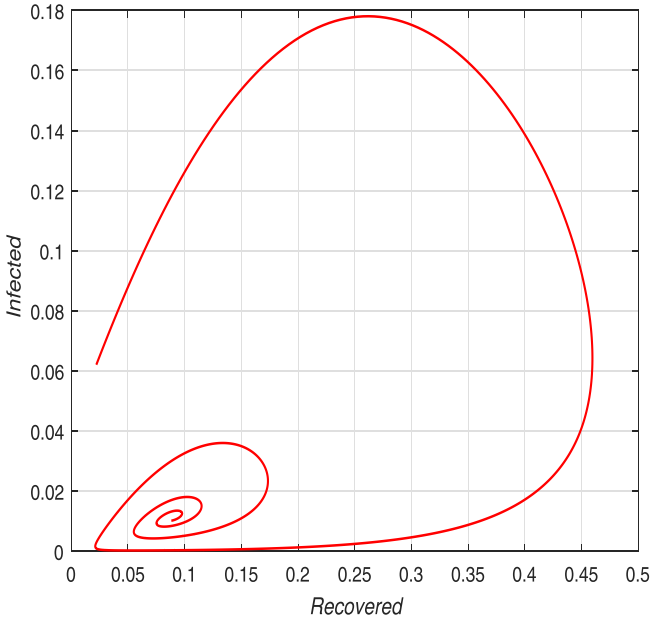

Fig. 11. Behaviour of the recovered and the infected people for Case 1 when $\sigma = 0.9$.

dealing with the fractional IVPs and DEs of the any kind (see [75,76]). Let us assume the following FDEs:

$$ {}^{\mathrm{LC}}D_t^{\sigma}\mathscr{S}_j(t) = f_j\left(t, \mathscr{S}_j(t)\right) \quad \text{and} \quad \mathscr{S}_j^{(k)}(0) = \mathscr{S}_{j0}^{(k)} \lceil \sigma \rceil \qquad \left(j \in \mathbb{N}\right), \tag{6.4} $$

where $\mathscr{S}_{j0}^{(k)}$ are irrational real numbers, $\sigma > 0$ and D_t^{σ} is the arbitrary derivative operator in the Liouville-Caputo style. This indeed is similar to the well-known Volterra integral equation:

$$ \mathscr{S}_j(t) = \sum_{n=0}^{\lceil \sigma \rceil - 1} \mathscr{S}_{j0}^{(n)} \frac{t^n}{n!} + \frac{1}{\Gamma(\sigma)} \int_0^t (t-\nu)^{\sigma-1} f_j\left(\nu, \mathscr{S}_j(\nu)\right) d\nu \quad \left(j \in \mathbb{N}\right). \tag{6.5} $$

We now clarify the required numerical solution of the nonlinear arbitrary-order SIR epidemic system by using the ABM method. Further, if we let $h = \frac{1-0}{\widehat{m}}, t_n = nh$ and $n = 0, 1, 2, \cdots, \widehat{m}$, then the correcter costs are characterized as follows:

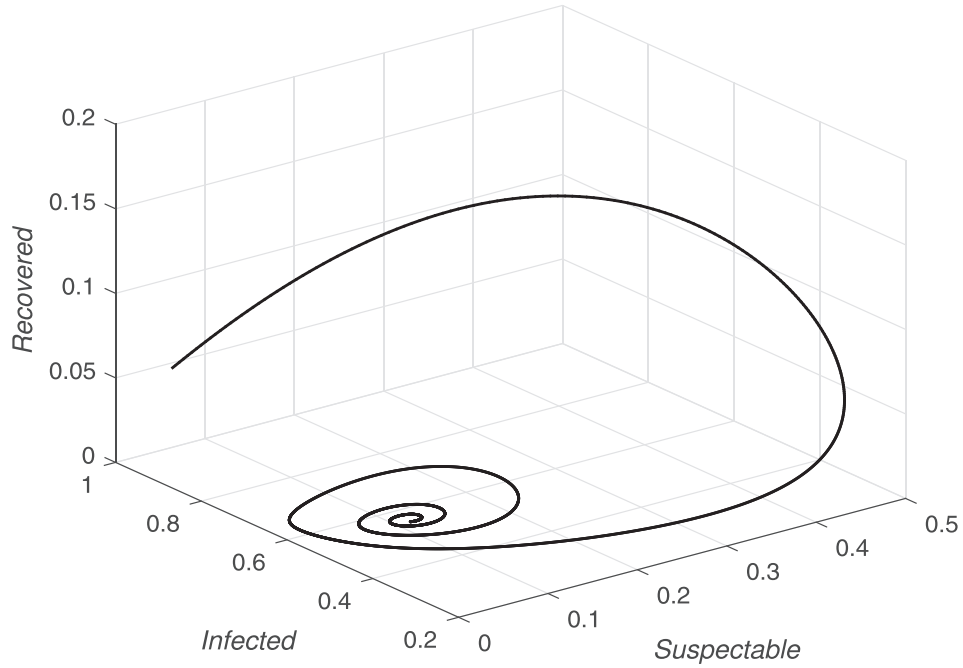

Fig. 12. Behaviour of the susceptible, infected and recovered peoples for Case 1 when $\sigma = 0.9$.

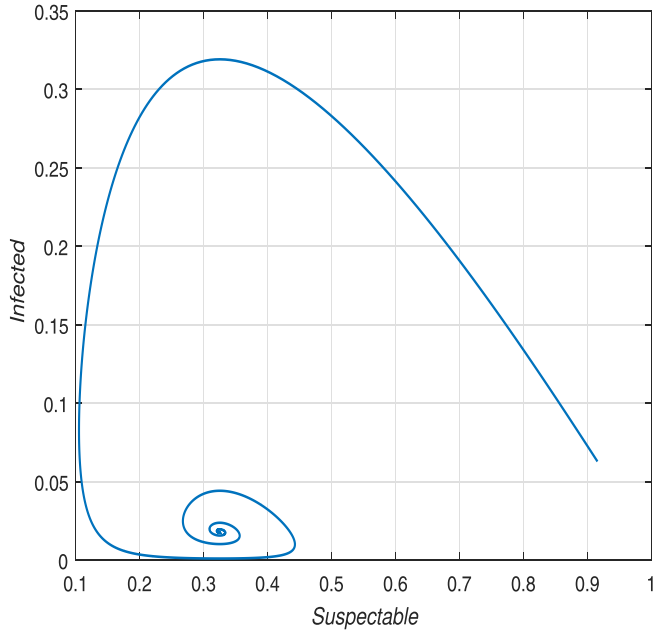

Fig. 13. Behaviour of the susceptible and the infected people for Case 2 when $\sigma = 0.9$.

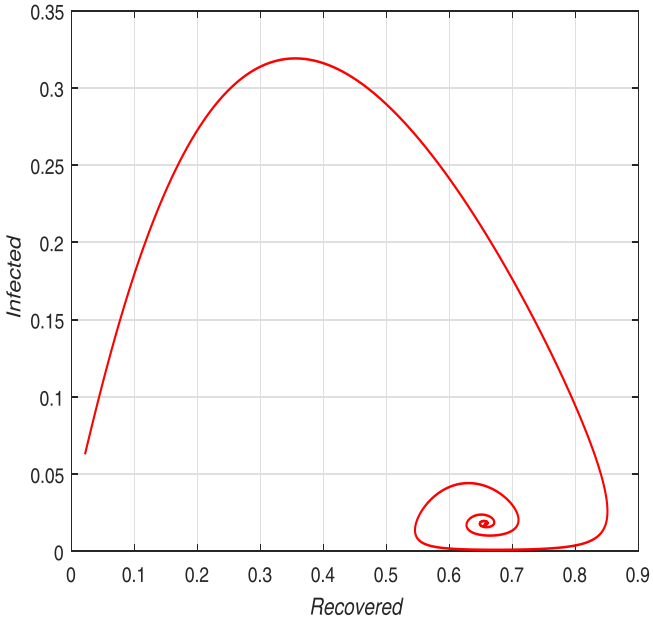

Fig. 14. Behaviour of the recovered and the infected people for Case 2 when $\sigma = 0.9$.

$$\mathscr{S}_{n+1} = \mathscr{S}\left(0\right) + \frac{h^{\sigma}}{\Gamma(\sigma+2)}\{(1-P)b - \beta\mathscr{S}^{p}_{n+1}\mathscr{I}^{p}_{n+1} - b\mathscr{S}^{p}_{n+1}\} \frac{h^{\sigma}}{\Gamma(\sigma+2)}\sum_{j=0}^{n}\alpha_{j,n+1}\cdot\{(1-P)b - \beta\mathscr{S}_{j}\mathscr{I}_{j} - b\mathscr{S}_{j}\},$$

$$\mathscr{I}_{n+1} = \mathscr{I}\left(0\right) + \frac{h^{\sigma}}{\Gamma(\sigma+2)}\{\beta\mathscr{S}^{p}_{n+1}\mathscr{I}^{p}_{n+1} - (\delta + \mu)\mathscr{I}^{p}_{n+1}\} + \frac{h^{\sigma}}{\Gamma(\sigma+2)}\sum_{j=0}^{n}\alpha_{j,n+1}\left[\beta\mathscr{S}_{j}\mathscr{I}_{j} - (\delta+\mu)\mathscr{I}_{j}\right]$$

and

$$\mathscr{R}_{n+1} = \mathscr{R}\left(0\right) + \frac{h^{\sigma}}{\Gamma(\sigma+2)}\left(Pb + \delta\mathscr{I}^{p}_{n+1} - \mu\mathscr{R}^{p}_{n+1}\right) + \frac{h^{\sigma}}{\Gamma(\sigma+2)}\sum_{j=0}^{n}\alpha_{j,n+1}\left(Pb + \delta\mathscr{I}_{j} - \mu\mathscr{R}_{j}\right).$$

Thus, clearly, the respective predictor values are characterizes in the following way:

$$\mathscr{S}^{p}_{n+1} = \mathscr{S}\left(0\right) + \frac{1}{\Gamma(\sigma)}\sum_{j=0}^{n}\beta_{j,n+1}\{(1-P)b - \beta\mathscr{S}_{j}\mathscr{I}_{j} - b\mathscr{S}_{j}\},$$

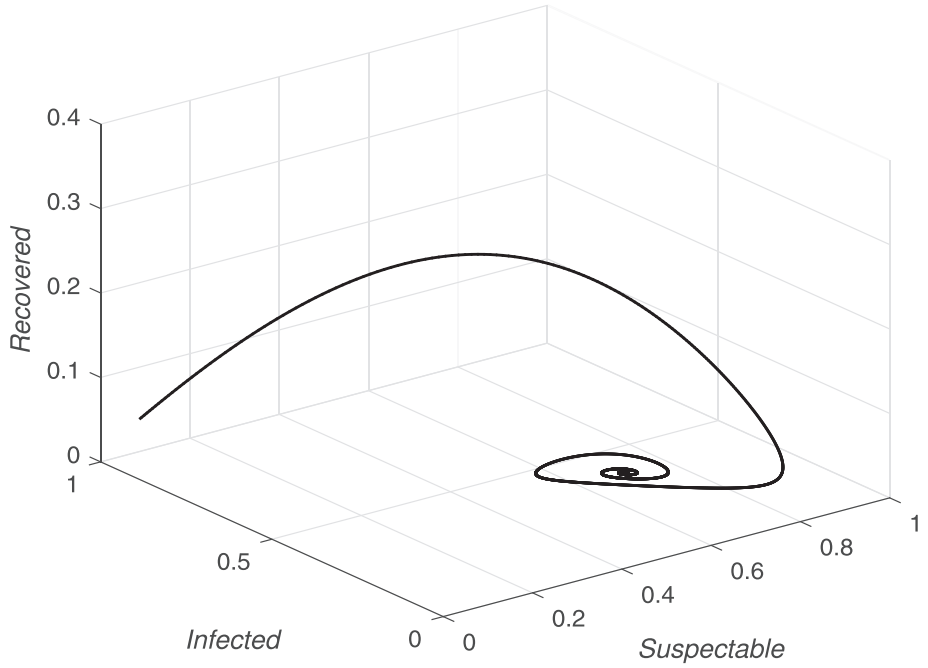

Fig. 15. Behaviour of the susceptible, infected and recovered peoples for Case 2 when $\sigma = 0.9$.

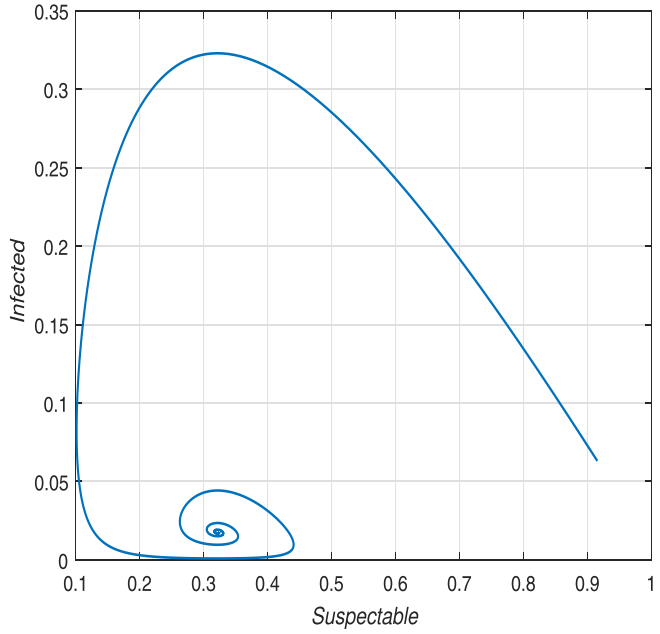

Fig. 16. Behaviour of the susceptible and the infected people for Case 3 when $\sigma = 0.9$.

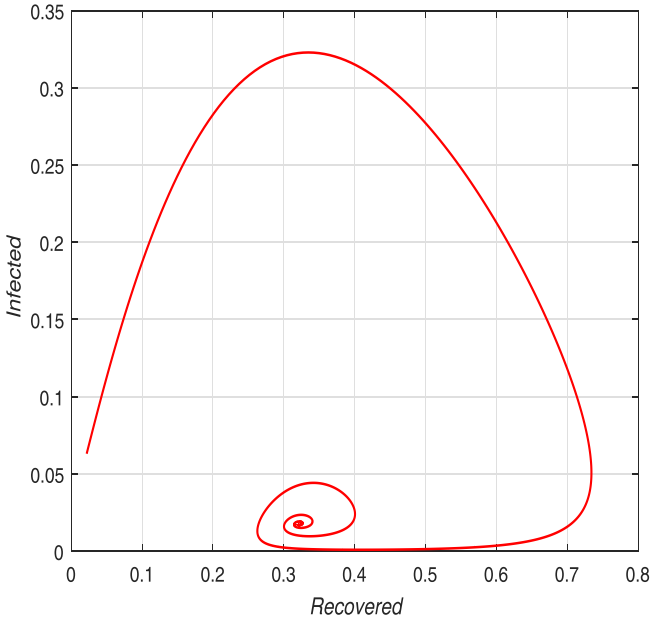

Fig. 17. Behaviour of the recovered and the infected people for Case 3 when $\sigma = 0.9$.

$$\mathscr{I}^{p}_{n+1} = I\left(0\right) + \frac{1}{\Gamma(\sigma)} \sum_{j=0}^{n} \beta_{j,n+1} \left\{\beta \mathscr{S}_j \mathscr{I}_j - \left(\delta + \mu\right) \mathscr{I}_j\right\}$$

and

$$\mathscr{R}^{p}_{n+1} = \mathscr{R}\left(0\right) + \frac{1}{\Gamma(\sigma)} \sum_{j=0}^{n} \beta_{j,n+1} \left(Pb + \delta \mathscr{I}_j - \mu \mathscr{R}_j\right),$$

where

$$\sigma_{j,n+1} = \begin{cases} n^{\sigma+1} - \left(n - \sigma\right)(n+1)^{\sigma} & (j = 0) \\ (n-j+2)^{\sigma+1} + (n-j)^{\sigma+1} - 2(n-j+1)^{\sigma+1} & (0 \leqslant j \leqslant n) \\ 1 & (j = 1), \end{cases}$$

and

$$\beta_{j,n+1} = \frac{h^{\sigma}}{\sigma} \left\{(n+1-j)^{\sigma} - (n-j)^{\sigma}\right\} \qquad \left(0 \leqslant j \leqslant n\right).$$

By using the techniques as detailed above, we have plotted various numerical results graphically.

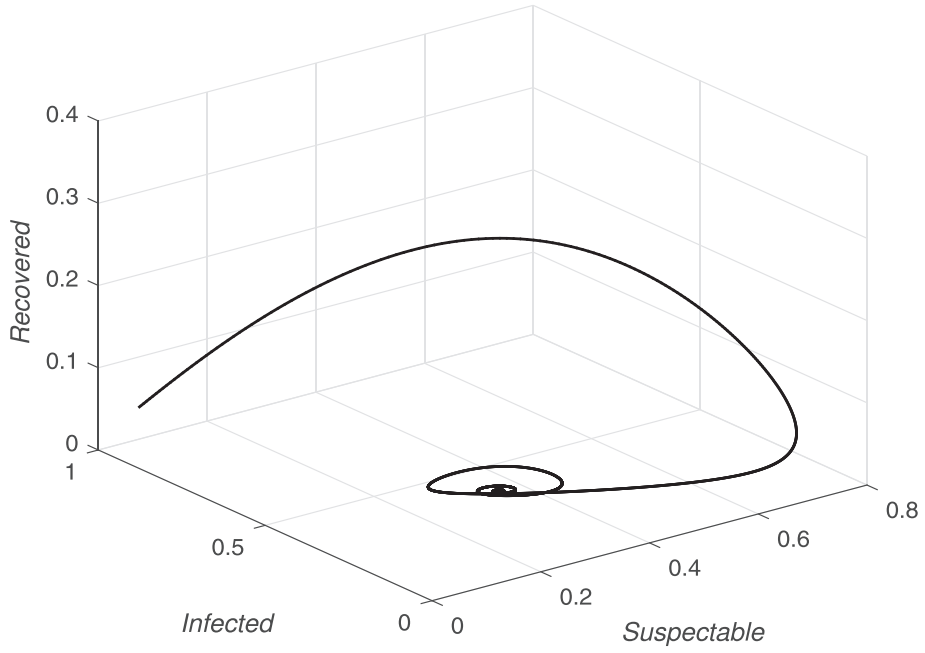

Fig. 18. Behaviour of the susceptible, infected and recovered peoples for Case 3 when $\sigma = 0.9$.

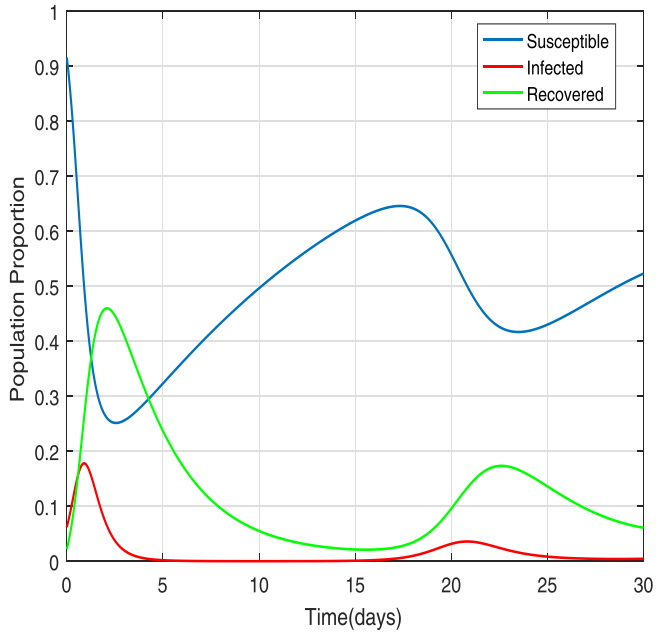

Fig. 19. Behaviour of the susceptible, infected and recovered peoples w.r.t. time for Case 1 when $\sigma = 1$.

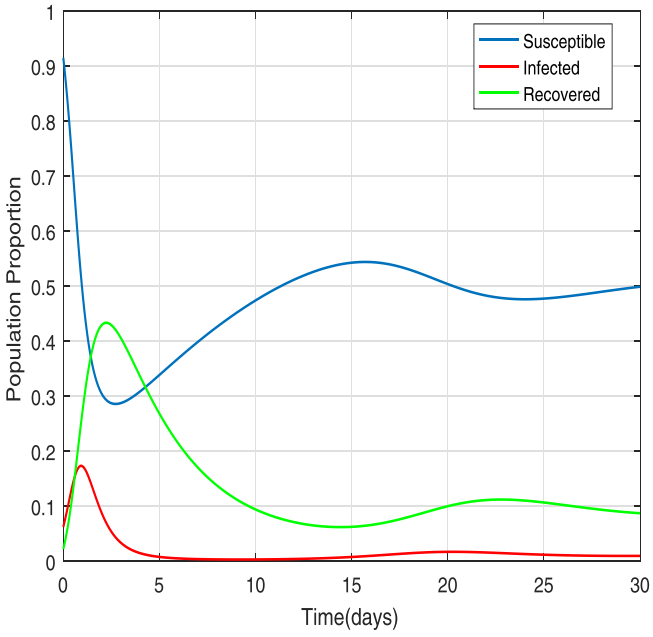

Fig. 20. Behaviour of the susceptible, infected and recovered peoples w.r.t. time for Case 1 when $\sigma = 0.95$.

Numerical investigations and associated discussions

The principal purpose of this part is to illustrate various numerical results by using the LAWM and ABM results of an arbitrary-order SIR epidemic model for many values of the order σ. The numerical simulations and behaviours of the susceptible, infected and recovered peoples in the arbitrary-order SIR epidemic system are depicted by means of Figs. 1–33. Figs. 1–3, in particular, show the 2D comparison between the achieved results by adopting the LAWM and ABM mechanisms. It is noticed from the behaviour of Fig. 1 that the rate of susceptible community almost similar by suggested numerical schemes and the rate of such community are decreasing according time. Fig. 1 indicate the comparison between susceptible community with respect to time at $M = 3, k = 6, \sigma = 1$ by adopting the LAWM and ABM methods. Fig. 2 indicate the comparison between infected community with respect to time at $M = 3, k = 6, \sigma = 1$ by adopting suggested numerical schemes. From the behaviour of Fig. 2, it is be observed from figure that the behaviours of infected community are identical by adopting suggested schemes in arbitrary-order SIR system. Also, we have observed that number of infected community are first increasing very fast according time. Further, we have observed through Fig. 3 that the number of recovered community are increasing with respect to time in the suggested SIR system of arbitrary order. Further, we observe that the achieved results $\mathscr{S}_{LAWM}(t)$, $\mathscr{I}_{LAWM}(t)$, $\mathscr{R}_{LAWM}(t)$, as well as $\mathscr{S}_{ABM}(t)$,$\mathscr{I}_{ABM}(t)$ and

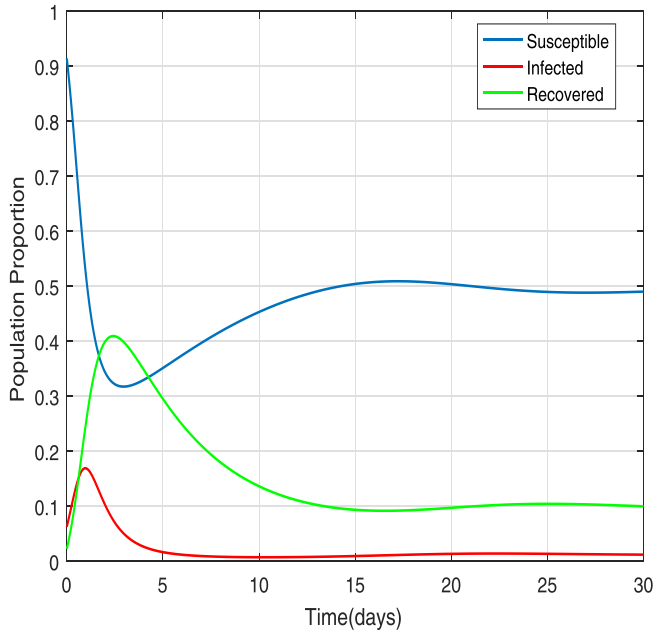

Fig. 21. Behaviour of the susceptible, infected and recovered peoples w.r.t. time for Case 1 when $\sigma = 0.90$.

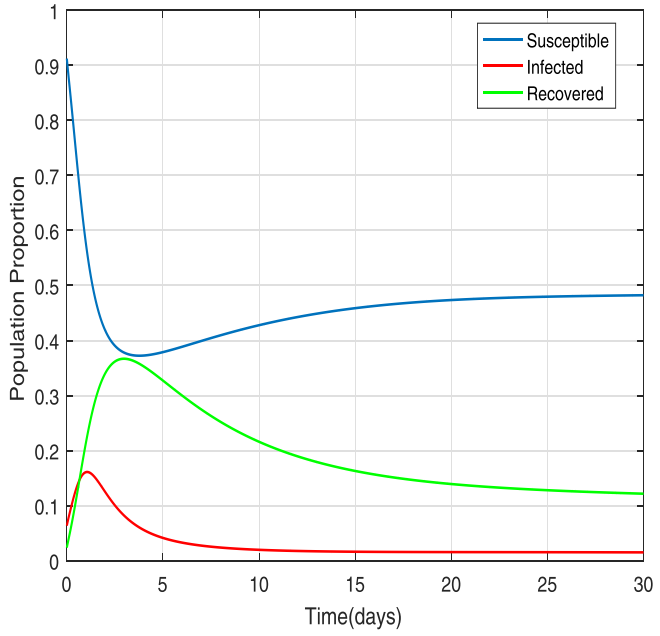

Fig. 22. Behaviour of the susceptible, infected and recovered peoples w.r.t. time for Case 1 when $\sigma = 0.80$.

$\mathscr{R}_{ABM}(t)$, are remarkably close to each other.

Moreover, our main focus is to find the accuracy between the achieved results by using the LAWM and ABM mechanisms. With this target in view, we have found the absolute error between the obtained results $S_{LAWM}(t), \mathscr{I}_{LAWM}(t), \mathscr{R}_{LAWM}(t)$, and $\mathscr{S}_{ABM}(t), \mathscr{I}_{ABM}(t), \mathscr{R}_{ABM}(t)$, respectively. Therefore, we assume the absolute error function to be characterized as follows:

$$AE_i^1(t) = \left|\mathscr{S}_{LAWM}(t) - \mathscr{S}_{ABM}(t)\right|, \quad (i \in \mathbb{N}),$$

$$AE_i^2(t) = \left|\mathscr{I}_{LAWM}(t) - \mathscr{I}_{ABM}(t)\right|, \quad (i \in \mathbb{N}),$$

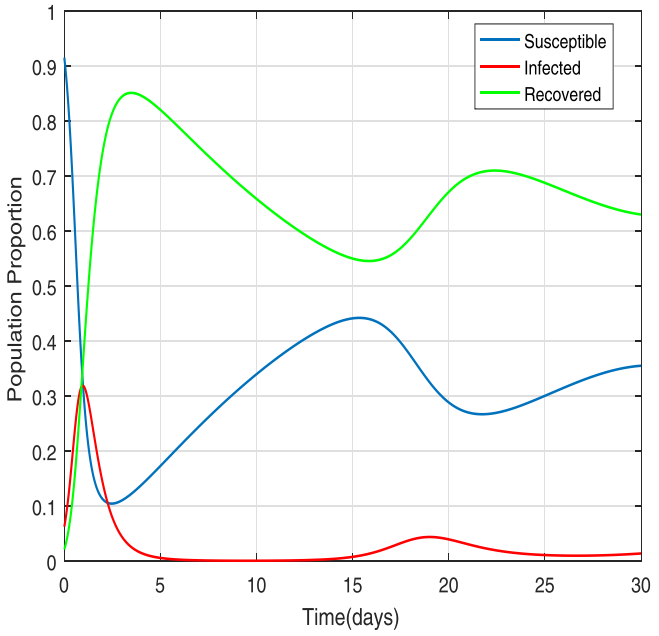

Fig. 23. Behaviour of the susceptible, infected and recovered peoples w.r.t. time for Case 2 when $\sigma = 1$.

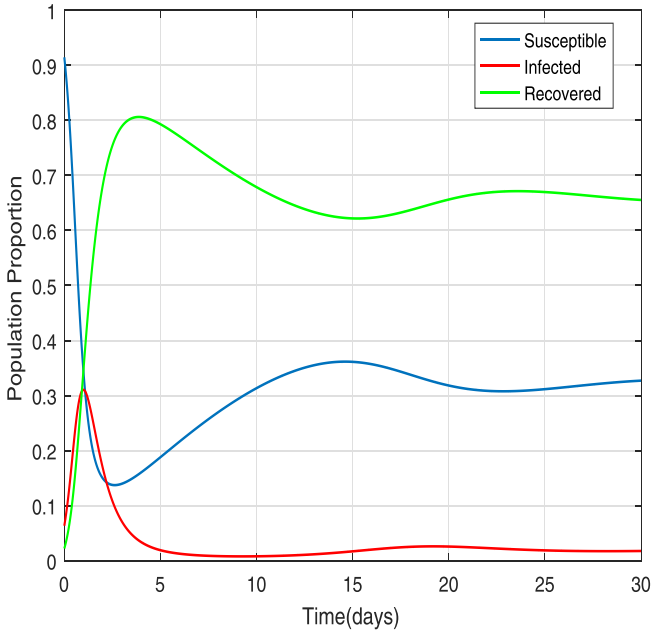

Fig. 24. Behaviour of the susceptible, infected and recovered peoples w.r.t. time for Case 2 when $\sigma = 0.95$.

and

$$AE_i^3(t) = \left|\mathscr{R}_{LAWM}(t) - \mathscr{R}_{ABM}(t)\right| \qquad (i \in \mathbb{N}),$$

where $\mathscr{S}_{LAWM}(t), \mathscr{S}_{ABM}(t), \mathscr{I}_{LAWM}(t), \mathscr{I}_{ABM}(t), \mathscr{R}_{LAWM}(t)$ and $\mathscr{R}_{ABM}(t)$ are the achieved results by using the Laguerre wavelet operational matrix mechanism and the ABM mechanism. All of the achieved results are approximately the same if

$$\lim_{i\to\infty}\left\{AE_i^1, AE_i^2, AE_i^3\right\} = \left\{0, 0, 0\right\}.$$

Also, the 2D presentation of the absolute errors AE_i^1, AE_i^2 and AE_i^3

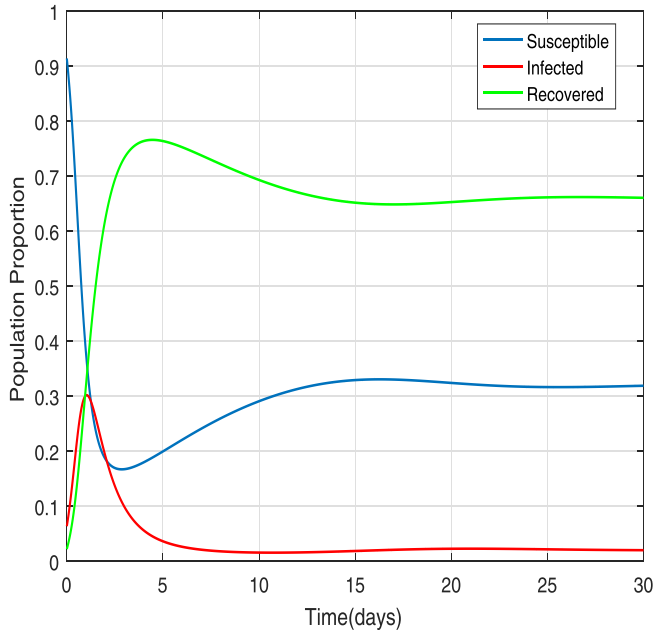

Fig. 25. Behaviour of the susceptible, infected and recovered peoples w.r.t. time for Case 2 when $\sigma = 0.90$.

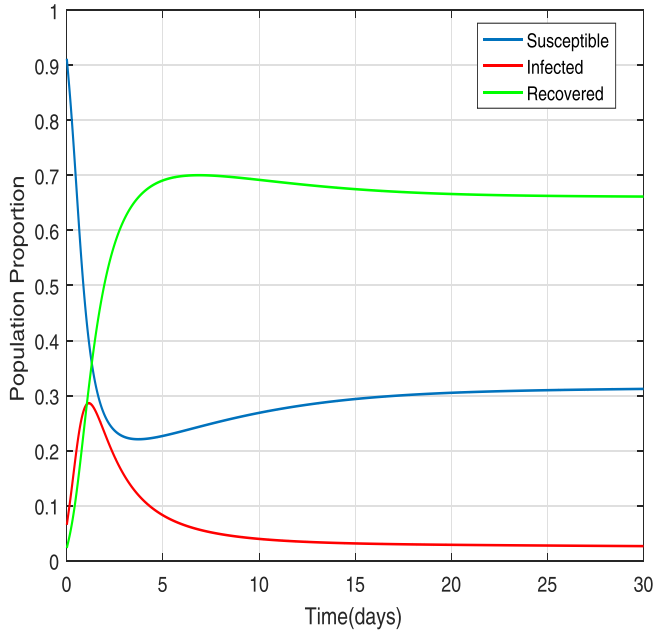

Fig. 26. Behaviour of the susceptible, infected and recovered peoples w.r.t. time for Case 2 when $\sigma = 0.80$.

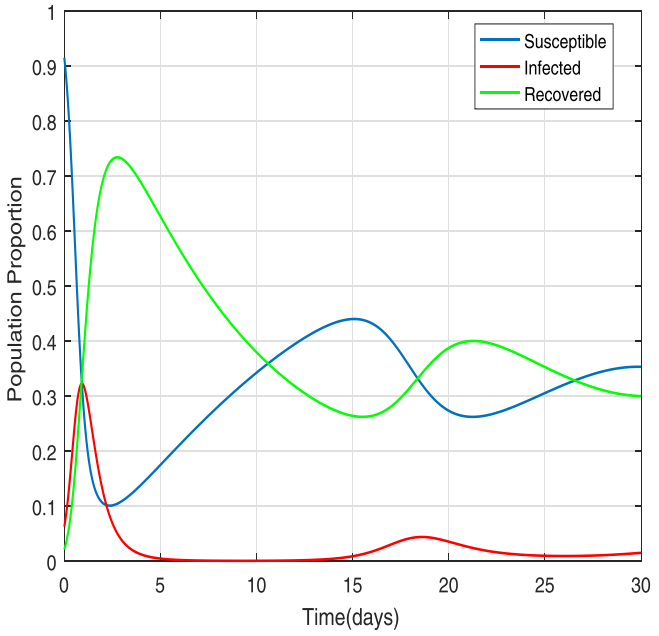

Fig. 27. Behaviour of the susceptible, infected and recovered peoples w.r.t. time for Case 3 when $\sigma = 1$.

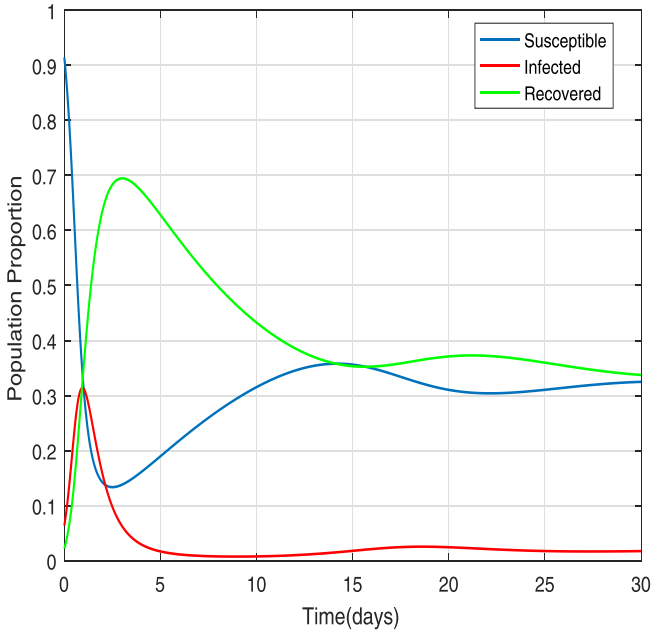

Fig. 28. Behaviour of the susceptible, infected and recovered peoples w.r.t. time for Case 3 when $\sigma = 0.95$.

between the obtained results is depicted by means of Figs. 4–6. The AE_i^1, AE_i^2 and AE_i^3 express the fact that we have accomplished an enhanced level of integrity between the achieved results by using the suggested mechanisms. We can thus obtain the enhanced level integrity between the produced results by enlarging the values of $i \in \mathbb{N}$.

For the reliable investigations, various evaluations is made for various value of arbitrary order. Furthermore, we have examined the behaviours of the susceptible, infected and recovered peoples through Figs. 7–9 for different value of arbitrary order $\sigma = 0.5, 0.60, 0.7, 0.80, 0.9$ in SIR system by adopting LAWM and ABM methods. It is also to be emphasized that we have observed high percentage of infected population at the primary stage of infection but after certain time percentage of infected population density become slower. Further, we have observed that the recovery percentage was slow at primary stage but recovery rate is high after a certain time. The comparative analysis between the susceptible, infected and recovered peoples in the arbitrary SIR system have been shown together graphically at different values of arbitrary order. The behaviours of the susceptible, infected and recovered (SIR) people are illustrated in Figs. 7–9 for various values of the order σ. According to our graphical study, we can say that the number of the susceptible people are contentiously deceasing while the numbers of the infected and recovered peoples are increasing with respect to time t for various values of the arbitrary order σ.

Further, the numerical simulations for chaotic behaviours of the

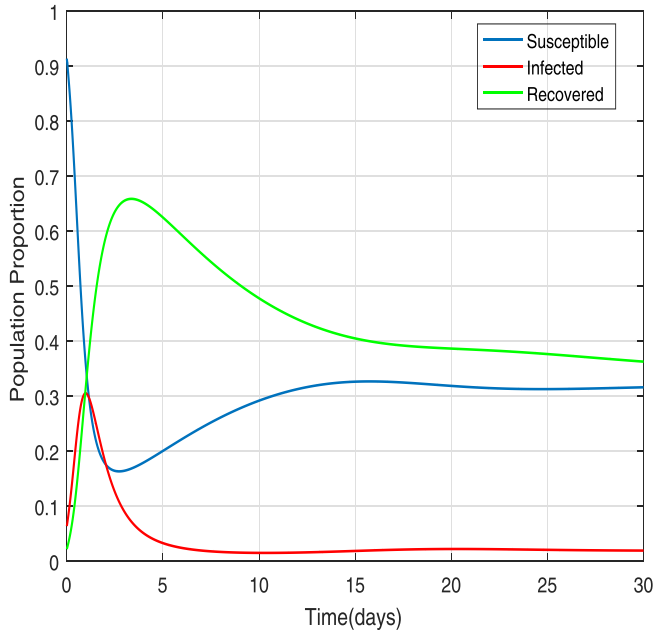

Fig. 29. Behaviour of the susceptible, infected and recovered peoples w.r.t. time for Case 3 when $\sigma = 0.90$.

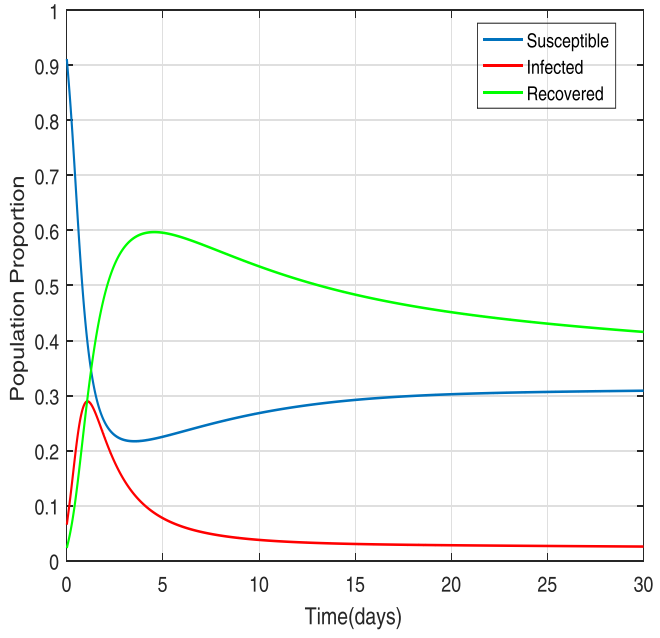

Fig. 30. Behaviour of the susceptible, infected and recovered peoples w.r.t. time for Case 3 when $\sigma = 0.80$.

susceptible, infected and recovered (SIR) people of the arbitrary -order SIR epidemic system are categorized in three various cases, Case 1, Case 2 and Case 3, which are clearly mentioned in Table 1. The simulation results demonstrate that chaos does indeed occur in the SIR epidemic system with a arbitrary order σ. Figs. 10–18 show various chaotic behaviours of the susceptible, infected and recovered peoples of the arbitrary -order SIR system by adopting the ABM mechanism. The comparative chaotic behaviours between susceptible and infected peoples are depicted in Fig. 10 and the comparative chaotic behaviours between the infected and recovered peoples are illustrated in Fig. 11 for Case 1 when $\sigma = 0.9$. Furthermore, the comparative chaotic behaviours between all susceptible, infected and recovered peoples are illustrated

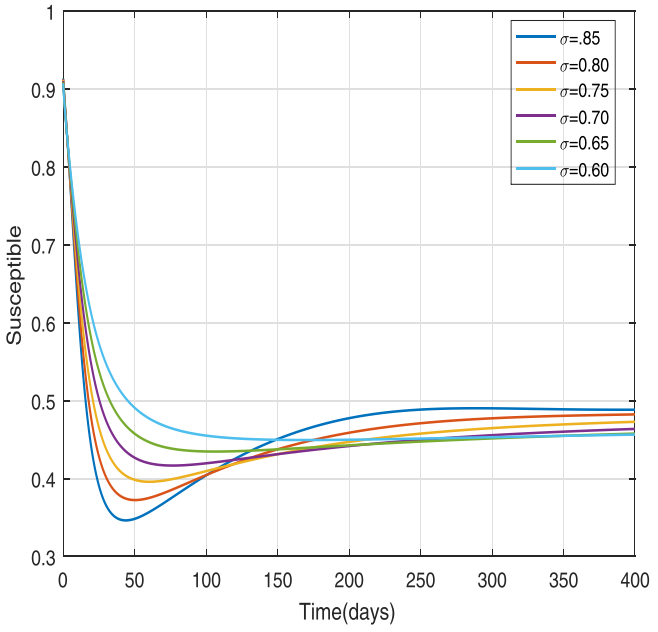

Fig. 31. Behaviour of the susceptible people for different values of σ.

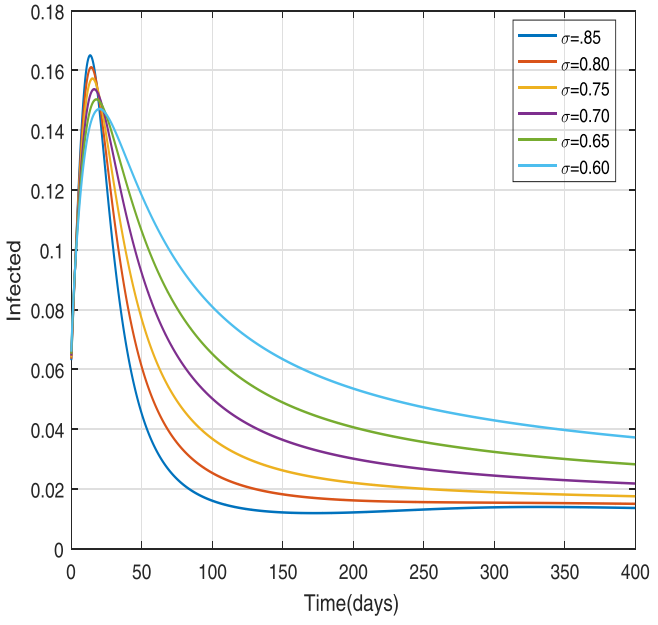

Fig. 32. Behaviour of the infected people for different values of σ.

by means of Fig. 12 for Case 1 when $\sigma = 0.9$. Similarly, Figs. 13–18 represent the comparative chaotic behaviours between susceptible, infected and recovered peoples for Case 2 and Case 3.

Furthermore, the behaviour of the susceptible, infected and recovered peoples in the arbitrary-order SIR epidemic system is demonstrated for various values of the arbitrary order σ in several cases. Figs. 19–33 represent the behaviours of the susceptible, infected and recovered peoples for different values of the arbitrary order σ. The behaviors of the susceptible, infected and recovered peoples w.r.t. time for Case 1 are depicted in Figs. 19–22 for various values of the order $\sigma = 1, 0.95, 0.90$ and $\sigma = 0.80$. Similarly, the behaviors of the susceptible, infected and recovered peoples w.r.t. time for Cases 2 and 3 are depicted by means of Figs. 23–33 for different values of $\sigma = 1, 0.95, 0.90$ and $\sigma = 0.80$. We have considered a number of parameters for the numerical simulation of

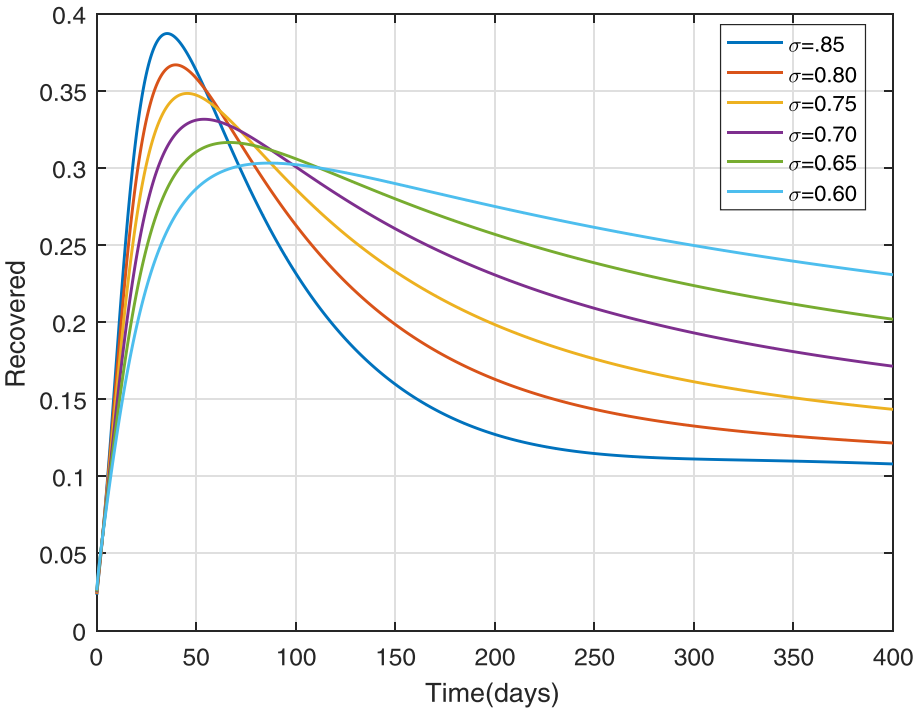

Fig. 33. Behaviour of the recovered people for different values of σ.

Table 1
Case study.

Parameters	P	b	β	δ	μ
Case 1	0.05	0.01	0.8	0.35	0.0.05
Case 2	0.2	0.01	0.8	0.25	0.01
Case 3	0.2	0.01	0.84	0.25	0.02

Eq. (1.2).

Summary and conclusions

Now-a-days researches on dynamic models of mathematical biology, population dynamics, epidemiology, evolution, immunology, morphogenesis, and pattern formation are remarkably popular research areas of applied mathematics. Due to their popularity, we examine the behaviours of famous arbitrary -order susceptible-infected- recovered (SIR) epidemic of childhood diseases by means of two numerical schemes. In this study, we have obtained numerical solutions of a arbitrary-order SIR model by adopting the Laguerre wavelet method and the ABM mechanism. Further, we have investigated the dynamical behaviours of the arbitrary-order SIR epidemic model by adopting the Adams–Bashforth-Moulton (ABM) schemes. Numerical results and graphs show that chaos exists in the arbitrary-order SIR epidemic system for positive integer and arbitrary orders. It is clear from our study that the idea of fractional-order nonlinear system, which simultaneously posses memory and chaos, is potentially useful for offering greater insights towards the understanding of the complex behaviours of various biological systems. In this article, we have successfully derives the Laguerre wavelets based operational matrix of arbitrary integration. We have also used it to solve a SIR epidemic system of an arbitrary order. The achieved solutions and results are convergent to the existing solution available in the literature. It is worth mentioning here that the results obtained by the LAW method agree well with the numerical solutions obtained by using ABM scheme. Convergence and error analysis assert the validity of suggested technique.

The behaviours of the susceptible, infected and recovered (SIR) people have been depicted and illustrated graphically for positive integer and fractional orders. We have also analysed the chaotic behaviours of the susceptible, infected and recovered (SIR) people in attractive and descriptive ways. All numerical and graphical results are found to be almost the same in our less computational work here as those achieved by other numerical and analytical methods. Moreover, our achieved computational and numerical results illustrate the validity and accuracy of the scheme when compared to other existing processes. Finally, we conclude that the nominated Laguerre wavelet mechanism is a promising tool for determining and analyzing both linear and nonlinear dynamical systems of biological and medical sciences.

Scopes and motivations for future works

The new non-singular and the newly-developed Atangana-Baleanu (AB), proportional Liouville-Caputo (PLC) and constant proportional Liouville-Caputo (CPLC) operators of fractional calculus are established operators, but these operators are not yet formulated with the wavelet methods (see [40,48]). So, one has great opportunity to explore their applications to the real-world problems by using various wavelet methods in conjunction with each of these newly-developed fractional-calculus operators. These suggested forthcoming works will have the potential to check the performance of each of these newly-developed Atangana-Baleanu (AB), proportional Liouville-Caputo (PLC) and constant proportional Liouville-Caputo (CPLC) fractional-calculus operators on wavelet methods for nonlinear PDEs arising in various fields of the physical, biological, engineering, medical, and other applied sciences. Furthermore, one can find the chaotic behaviour of each of these biological models by analogously using the AB, PLC and CPLC fractional-calculus operators.

Declaration of Competing Interest

The authors declare that they have no known competing financial interests or personal relationships that could have appeared to influence the work reported in this paper.

References

[1] Martcheva M. An introduction to mathematical epidemiology, Vol. 61. New York: Springer; 2015.
[2] Roberts M, Heesterbeek J. Mathematical models in epidemiology, Vol. 69. New York: Springer; 2019.
[3] Allen LJ, Brauer F, Van den Driessche P, Wu J. Mathematical epidemiology, Vol. 1945. New York: Springer; 2008.
[4] Ma Z, Li J. Dynamical modeling and analysis of epidemics. Singapore: World Scientific; 2009.
[5] Nátr J, Murray JD. Mathematical biology 1. An introduction. Photosynthetica 2002;40(3):414.
[6] Kermack WO, McKendrick AG. A contribution to the mathematical theory of epidemics. Proc R Soc Lond Ser A 1927;115(772):700–21.
[7] Selvam AGM, Vianny DA, Jacintha M. Stability in a fractional order SIR epidemic model of childhood diseases with discretization. In: Journal of Physics: Conference Series, Vol. 1139, IOP Publishing, 2018. p. 012009.
[8] Kumar S, Kumar R, Kumar D, Singh J, Baleanu D, Salimi M. An efficient numerical method for fractional SIR epidemic model of infectious disease by using Bernstein wavelets. Mathematics 2020;8(4):558.
[9] Ghanbari B, Kumar S, Kumar R. A study of behaviour for immune and tumor cells in immunogenetic tumour model with non-singular fractional derivative. Chaos Soliton Fractals 2020;133:109619.
[10] Ullah S, Khan MA, Farooq M. A new fractional model for the dynamics of the Hepatitis B virus using the Caputo-Fabrizio derivative. Eur Phys J Plus 2018;133 (6):237.
[11] Cardoso L, Dos Santos F, Camargo R. Analysis of fractional-order models for Hepatitis B. Comput Appl Math 2018;37(4):4570–86.
[12] Arafa A, Rida S, Khalil M. Solutions of fractional order model of childhood diseases with constant vaccination strategy. Math Sci Lett 2012;1(1):17–23.
[13] Shah SAA, Khan MA, Farooq M, Ullah S, Alzahrani EO. A fractional order model for Hepatitis B virus with treatment via Atangana-Baleanu derivative. Physica A 2020; 538:122636.
[14] Singh H, Dhar J, Bhatti HS, Chandok S. An epidemic model of childhood disease dynamics with maturation delay and latent period of infection. Model Earth Syst Environ 2016;2(2):79.
[15] Koca I. Analysis of rubella disease model with non-local and non-singular fractional derivatives. Int J Optim Control: Theor Appl (IJOCTA) 2017;8(1):17–25.
[16] Srivastava HM, Günerhan H. Analytical and approximate solutions of fractional-order susceptible-infected-recovered epidemic model of childhood disease. Math Methods Appl Sci 2019;42(3):935–41.
[17] Haq F, Shahzad M, Muhammad S, Wahab HA, Ur Rahman G. Numerical analysis of fractional order epidemic model of childhood diseases. Discr Dyn Nat Soc 2017: 4057089.
[18] Almeida R, da Cruz AMB, Martins N, Monteiro MTT. An epidemiological MSEIR model described by the Caputo fractional derivative. Int J Dyn Control 2019;7(2): 776–84.
[19] Hethcote HW. The mathematics of infectious diseases. SIAM Rev 2000;42(4): 599–653.
[20] Ibeas A, Shafi M, Ishfaq M, Ali M. Vaccination controllers for SEIR epidemic models based on fractional order dynamics. Biomed Signal Process Control 2017;38: 136–42.
[21] Kumar S, Kumar R, Singh J, Nisar KS, Kumar D. An efficient numerical scheme for fractional model of HIV-1 infection of CD4+ T-Cells with the effect of antiviral drug therapy. Alexandria Eng J doi:10.1016/j.aej.2019.12.046.
[22] Srivastava VK, Awasthi MK, Kumar S. Numerical approximation for HIV infection of CD4+ T-Cells mathematical model. AIN Shams Eng J 2014;5(2):625–9.
[23] Makinde OD. Adomian decomposition approach to a epidemic model with constant vaccination strategy. Appl Math Comput 2007;184(2):842–8.
[24] Arqub OA, El-Ajou A. Solution of the fractional epidemic model by homotopy analysis method. J King Saud Univ Sci 2013;25(1):73–81.
[25] Ahmad A, Farman M, Ahmad M, Raza N, Abdullah M. Dynamical behavior of SIR epidemic model with non-integer time fractional derivatives: A mathematical analysis. Int J Adv Appl Sci 2018;5(1):123–9.
[26] Kumar R, Kumar S. A new fractional modelling on susceptible-infected-recovered equations with constant vaccination rate. Nonlinear Eng 2014;3(1):11–9.
[27] Angstmann CN, Henry BI, McGann AV. A fractional-order infectivity and recovery SIR model. Fractal Fractional 2017;1(1):11.
[28] Mouaouine A, Boukhouima A, Hattaf K, Yousfi N. A fractional order SIR epidemic model with nonlinear incidence rate. Adv Differ Eqs 2018;2018(1):1–9.
[29] Hasan S, Al-Zoubi A, Freihet A, Al-Smadi M, Momani S. Solution of fractional SIR epidemic model using residual power series method. Appl Math Inf Sci 2019;13(2): 1–9.
[30] Yang X-J, Baleanu D, Srivastava HM. Local fractional integral transforms and their applications. New York: Academic Press; 2015.
[31] Yang X-J. General fractional derivatives: Theory, methods and applications. Baton Roca, Florida: CRC Press; 2019.
[32] Das S. Functional fractional calculus. Switzerland: Springer Science & Business Media; 2011.
[33] Baleanu D, Kai D, Enrico S. Fractional calculus: models and numerical methods, Vol. 3. Singapore: World Scientific; 2012.
[34] Yildiz TA, Jajarmi A, Yildiz B, Baleanu D. New aspects of time fractional optimal control problems within operators with nonsingular kernel. Discr Contin Dyn Syst S 2020;13(3):407.
[35] Baleanu D, Jajarmi A, Mohammadi H, Rezapour S. A new study on the mathematical modelling of human liver with Caputo-Fabrizio fractional derivative. Chaos Solitons Fractals 2020;134:109705.
[36] Jajarmi A, Ghanbari B, Baleanu D. A new and efficient numerical method for the fractional modeling and optimal control of diabetes and tuberculosis co-existence. Chaos: Interdisc J Nonlinear Sci 2019;29(9):093111.
[37] Baleanu D, Jajarmi A, Sajjadi SS, Mozyrska D. A new fractional model and optimal control of a tumor-immune surveillance with non-singular derivative operator. Chaos: Interdisc J Nonlinear Sci 2019;29(8):083127.
[38] Jajarmi A, Arshad S, Baleanu D. A new fractional modelling and control strategy for the outbreak of dengue fever. Physica A Stat Mech Appl 2019;535:122524.
[39] Jajarmi A, Ghanbari B, Baleanu D. A new and efficient numerical method for the fractional modeling and optimal control of diabetes and tuberculosis co-existence. Chaos Interdisc J Nonlinear Sci 2019;29(9):093111.
[40] Atangana A, Baleanu D. New fractional derivatives with nonlocal and non-singular kernel: Theory and application to heat transfer model. Therm Sci 2016;20(2):1–7.
[41] Gao W, Ghanbari B, Baskonus HM. New numerical simulations for some real world problems with Atangana-Baleanu fractional derivative. Chaos Solitons Fractals 2019;128:34–43.
[42] Ravichandran C, Logeswari K, Jarad F. New results on existence in the framework of Atangana-Baleanu derivative for fractional integro-differential equations. Chaos Solitons Fractals 2019;125:194–200.
[43] Panda SK, Abdeljawad T, Ravichandran C. A complex valued approach to the solutions of Riemann-Liouville integral, Atangana-Baleanu integral operator and non-linear telegraph equation via fixed point method. Chaos Solitons Fractals 2020;130:109439.
[44] Akgül A. A novel method for a fractional derivative with non-local and non-singular kernel. Chaos Solitons Fractals 2018;114:478–82.
[45] Akgül A, Modanli M. Crank-Nicholson difference method and reproducing kernel function for third order fractional differential equations in the sense of Atangana-Baleanu Caputo derivative. Chaos Solitons Fractals 2019;127:10–6.
[46] Prakasha D, Veeresha P, Baskonus HM. Analysis of the dynamics of Hepatitis E virus using the Atangana-Baleanu fractional derivative. Eur Phys J Plus 2019;134 (5):241.
[47] Gao W, Veeresha P, Prakasha D, Baskonus HM, Yel G. New approach for the model describing the deathly disease in pregnant women using Mittag-Leffler function. Chaos Solitons Fractals 2020;134:109696.
[48] Baleanu D, Fernandez A, Akgül A. On a Fractional Operator Combining Proportional and Classical Differintegrals. Mathematics 2020;8(3):360.
[49] Wu G-C, Baleanu D. Chaos synchronization of the discrete fractional logistic map. Signal Process 2014;102:96–9.
[50] Smith L. Chaos: A very short introduction, Vol. 159. Oxford: Oxford University Press; 2007.
[51] Strogatz SH. Nonlinear dynamics and chaos with student solutions manual: With applications to physics, biology, chemistry, and engineering. Baton Roca, Florida: CRC Press; 2018.
[52] Kumar S, Kumar R, Cattani C, Samet B. Chaotic behaviour of fractional predator-prey dynamical system. Chaos Solitons Fractals 2020;135:109811.
[53] Razzaghi M, Yousefi S. The Legendre wavelets operational matrix of integration. Int J Syst Sci 2001;32(4):495–502.
[54] Shamsi M, Razzaghi M. Solution of Hallen's integral equation using multiwavelets. Comput Phys Commun 2005;168(3):187–97.
[55] Sontag ED. Lecture notes on mathematical systems biology. New Brunswick, New Jersey: Rutgers University; 2011.
[56] Lakestani M, Razzaghi M, Dehghan M. Semiorthogonal spline wavelets approximation for Fredholm integro-differential equations. Math Probl Eng 2006; 2006:96184.
[57] Beylkin G, Coifman R, Rokhlin V. Fast wavelet transforms and numerical Algorithms 1. Commun Pure Appl Math 1991;44(2):141–83.
[58] Iqbal MA, Saeed U, Mohyud-Din ST. Modified Laguerre wavelets method for delay differential equations of fractional-order. Egyptian J Basic Appl Sci 2015;2(1): 50–4.
[59] Shiralashetti S, Kumbinarasaiah S. Laguerre wavelets collocation method for the numerical solution of the Benjamin–Bona–Mohany equations. J Taibah Univ Sci 2019;13(1):9–15.
[60] Gümgüm S. Laguerre wavelet method for solving Troesch equation. Balikesir Üniversitesi Fen Bilimleri Enstitüsü Dergisi 2019;21(2):494–502.
[61] Shiralashetti S, Angadi L, Kumbinarasaiah S. Laguerre wavelet-Galerkin method for the numerical solution of one dimensional partial differential equations. Int J Math Appl 2018;55:939–49.
[62] Shiralashetti S, Kumbinarasaiah S. Theoretical study on continuous polynomial wavelet bases through wavelet series collocation method for nonlinear Lane-Emden type equations. Appl Math Comput 2017;315:591–602.
[63] Yuttanan B, Razzaghi M. Legendre wavelets approach for numerical solutions of distributed order fractional differential equations. Appl Math Model 2019;70: 350–64.
[64] Rahimkhani P, Ordokhani Y. A numerical scheme based on Bernoulli wavelets and collocation method for solving fractional partial differential equations with Dirichlet boundary conditions. Numer Methods Partial Differ Eqs 2019;35(1): 34–59.
[65] Srivastava HM, Shah FA, Abass R. An application of the Gegenbauer wavelet method for the numerical solution of the fractional Bagley-Torvik equation. Russ J Math Phys 2019;26(1):77–93.
[66] Srivastava M, Agrawal S, Das S. Synchronization of chaotic fractional order Lotka-Volterra system. Int J Nonlinear Sci 2012;13(4):482–94.

[67] Diethelm K, Ford NJ, Freed AD. Detailed error analysis for a fractional Adams method. Numer Algorith 2004;36(1):31–52.
[68] Cui Q, Xu J, Zhang Q, Wang K. An NSFD scheme for SIR epidemic models of childhood diseases with constant vaccination strategy. Adv Differ Eqs 2014;2014 (1):172.
[69] Akgül A. A new method for approximate solutions of fractional order boundary value problems. Neural Parallel Sci Comput 2014;22(1–2):223–37.
[70] Atangana KOA, Akgül A. Analysis of fractal fractional differential equations. Alexandria Eng J 2020;59(3):1117–34.
[71] Kilbas AA, Srivastava HM, Trujillo JJ. Theory and applications of fractional differential equations, Vol. 204. London and New York: Elsevier (North-Holland) Science Publishers, Amsterdam; 2006.
[72] Rainville ED. Special Functions. New York: Macmillan; 1971.
[73] Matignon D. Stability results for fractional differential equations with applications to control processing. In: Computational Engineering in Systems Applications, Vol. 2, Lille, France, 1996. p. 963–968.
[74] Srivastava M, Agrawal S, Vishal K, Das S. Chaos control of fractional order Rabinovich-Fabrikant system and synchronization between chaotic and chaos controlled fractional order Rabinovich-Fabrikant system. Appl Math Model 2014; 38(13):3361–72.
[75] Diethelm K, Ford NJ. Multi-order fractional differential equations and their numerical solution. Appl Math Comput 2004;154(3):621–40.
[76] Masjed-Jamei M, Moalemi Z, Srivastava HM, Area I. Some modified Adams-Bashforth methods based upon the weighted Hermite quadrature rules. Math Methods Appl Sci 2020;43(3):1380–98.